Table 1: List of previous gene transfer to the central nervous system with virus

	Year	Authors	Virus	No. of injected particles	Injecting site	Animals	Peak time (days)	Observation period (days)	Gene
1	1993	Bajocchi *et al.*	Ad	5×10^9 pfu	LV	SD rat	4	6	βgal
2	1995	Ooboshi *et al.*	Ad	1×10^9 pfu	CM	SD rat	1	7	βgal
3	1995	Betz *et al.*	Ad	Particle 1×10^9 pfu	LV	Rat	5	5	βgal
5	1998	Kitagawa *et al.*	Ad	2.5×10^9 pfu	LV	Gerbil	1	21	βgal
6	1998	Yang *et al.*	Ad	1×10^9 particle	LV	CD-1 mice	5	5	βgal
7	1998	Ghodsi *et al.*	Ad	2×10^7 pfu	LV CM	C57BL/6 mice	21	21	βgal
8	1998	Abe *et al.*	Ad	2.5×10^9 pfu	LV	Gerbil	7	21	βgal
9	2000	Davidson *et al.*	AAV	3×10^{10} pfu	LV	C57BL/6 mice	21	105	βgal
10	2000	Yagi *et al.*	Ad	Ad 5×10^7 pfu	LV	Gerbil	2, 4, 7	7	βgal
11	2000	Mao *et al.*	Ad	Unknown	LV	CD-1 mice	5	5	βgal
12	2002	Baekelandt *et al.*	HIV-1	Unknown	LV	Mice	Unknown	Unknown	GFP
13	2002	Lin *et al.*	Ad	1×10^7 pfu	LV	LE rat	3	3	GFP
14	2003	Matsuoka *et al.*	Ad	2×10^8 pfu	LV	Gerbil	2	7	βgal
15	2003	Shirakura *et al.*	SeV	1×10^9 pfu	LV	Gerbil	4	7	GFP
16	2000	Driesse *et al.*	Ad	7.4×10^9 pfu	LV	Monkey	(–)	21	(–)
17	2000	Driesse *et al.*	Ad	5×10^9 pfu	LV	Rat	(–)	16	(–)
18	2000	Muzzin *et al.*	Ad	3×10^8 pfu	LV	Zucker	Rat	9	GFP

Ad=adenovirus, pfu=plaque forming units, LV=lateral ventricle, β-gal=β-galactosidease, GFP=green fluorescent protein, CM=cisterna magna, AAV=adenoassociated virus; HIV-1=human immunodeficiency virus, SeV=Sendai virus.

atrophy or hydrocephalus. Hydrocephalus in humans is often accompanied by periventricular lucency, indicating that the destruction of the ependymal layer permits influx of CSF from the ventricle to the brain parenchyma[44]. In our study, we observed edematous changes in the center of the hemisphere, but degenerative changes were apparent in the external capsule. Therefore, we speculate that the ventricles were compensatory dilated after degeneration of the neural fibers.

In conclusion, it is important to take this diffuse encephalo-ventriculitis into consideration for the clinical application of gene transfer into the ependymal cells or subarachnoid space.

ACKNOWLEDGEMENTS

This study was supported in part by Research Grants (15390433) from the Ministry of Education, Culture, Sports, Science and Technology of Japan.

REFERENCES

1 Wright JL, Merchant RE. Blood-brain barrier changes following intracerebral injection of human recombinant tumor necrosis factor-alpha in the rat. *J Neurooncol* 1994; **20**: 17–25
2 Kern MA, Bamborschke S, Nekic M, *et al.* Concentrations of hepatocyte growth factor in cerebrospinal fluid under normal and different pathological conditions. *Cytokine* 2001; **14**: 170–176
3 Pan W, Kastin AJ. Interactions of cytokines with the blood-brain barrier: Implications for feeding. *Curr Pharm Des* 2003; **9**: 827–831
4 Baker D, Hankey DJ. Gene therapy in autoimmune, demyelinating disease of the central nervous system. *Gene Ther* 2003; **10**: 844–853
5 Ooboshi H, Welsh MJ, Rios CD, *et al.* Adenovirus-mediated gene transfer in vivo to cerebral blood vessels and perivascular tissue. *Circ Res* 1995; **77**: 7–13
6 Viola JJ, Ram Z, Walbridge S, *et al.* Adenovirally mediated gene transfer into experimental solid brain tumors and leptomeningeal cancer cells. *J Neurosurg* 1995; **82**: 70–76
7 Shimamura M, Sato N, Oshima K, *et al.* Novel therapeutic strategy to treat brain ischemia: Overexpression of hepatocyte growth factor gene reduced ischemic injury without cerebral edema in rat model. *Circulation* 2004; **109**: 424–431
8 Le Gal La Salle G, Robert JJ, Berrard S, *et al.* An adenovirus vector for gene transfer into neurons and glia in the brain. *Science* 1993; **259**: 988–990
9 Breakefield XO. Gene delivery into the brain using virus vectors. *Nature Genet* 1993; **3**: 187–189
10 Bajocchi G, Feldman SH, Crystal RG, *et al.* Direct in vivo gene transfer to ependymal cells in the central nervous system using recombinant adenovirus vectors. *Nature Genet* 1993; **3**: 229–234
11 Yoon SO, Lois C, Alvirez M, *et al.* Adenovirus-mediated gene delivery into neuronal precursors of the adult mouse brain. *Proc Natl Acad Sci USA* 1996; **93**: 11974–11979
12 Kitagawa H, Setoguchi Y, Fukuchi Y, *et al.* DNA fragmentation and HSP72 gene expression by adenovirus-mediated gene transfer in postischemic gerbil hippocampus and ventricle. *Metab Brain Dis* 1998; **13**: 211–223
13 Yang GY, Liu XH, Kadoya C, *et al.* Attenuation of ischemic inflammatory response in mouse brain using an adenoviral vector to induce overexpression of interleukin-1 receptor antagonist. *J Cereb Blood Flow Metab* 1998; **18**: 840–847
14 Abe K, Kitagawa H, Setoguchi Y. Temporal profile of adenovirus-mediated *E. coli* lacZ gene expression in normal and post-ischemic gerbil hippocampus and ventricle. *Neurol Res* 1998; **20**: 689–696
15 Driesse MJ, Kros JM, Avezaat CJ, *et al.* Distribution of recombinant adenovirus in the cerebrospinal fluid of nonhuman primates. *Hum Gene Ther* 1999; **10**: 2347–2354
16 Davidson BL, Stein CS, Heth JA, *et al.* Recombinant adeno-associated virus type 2, 4, and 5 vectors: Transduction of variant cell types and regions in the mammalian central nervous system. *Proc Natl Acad Sci USA* 2000; **97**: 3428–3432
17 Yagi T, Maeda M, Tanaka A, *et al.* Detection of the exogenous hGDNF in gerbils under the treatment with AxCAhGDNF adenoviral vector. *Brain Res Brain Res Protoc* 2001; **8**: 88–98
18 Lin H, Lin TN, Cheung WM, *et al.* Cyclooxygenase-1 and bicistronic cyclooxygenase-1/prostacyclin synthase gene transfer protect against ischemic cerebral infarction. *Circulation* 2002; **105**: 1962–1969
19 Shirakura M, Fukumura M, Inoue M, *et al.* Sendai virus vector-mediated gene transfer of glial cell line-derived neurotrophic factor prevents delayed neuronal death after transient global ischemia in gerbils. *Exp Anim* 2003; **52**: 119–127

Circulation
JOURNAL OF THE AMERICAN HEART ASSOCIATION

American Heart Association®
Learn and Live℠

Postinfarction Gene Therapy Against Transforming Growth Factor-ß Signal Modulates Infarct Tissue Dynamics and Attenuates Left Ventricular Remodeling and Heart Failure

Hideshi Okada, Genzou Takemura, Ken-ichiro Kosai, Yiwen Li, Tomoyuki Takahashi, Masayasu Esaki, Kentaro Yuge, Shusaku Miyata, Rumi Maruyama, Atsushi Mikami, Shinya Minatoguchi, Takako Fujiwara and Hisayoshi Fujiwara

Circulation 2005;111;2430-2437; originally published online May 2, 2005;
DOI: 10.1161/01.CIR.0000165066.71481.8E
Circulation is published by the American Heart Association. 7272 Greenville Avenue, Dallas, TX 72514
 Print ISSN: 0009-7322. Online ISSN: 1524-4539

Postinfarction Gene Therapy Against Transforming Growth Factor-β Signal Modulates Infarct Tissue Dynamics and Attenuates Left Ventricular Remodeling and Heart Failure

Hideshi Okada, MD; Genzou Takemura, MD, PhD; Ken-ichiro Kosai, MD, PhD; Yiwen Li, MD, PhD; Tomoyuki Takahashi, PhD; Masayasu Esaki, MD; Kentaro Yuge, MD, PhD; Shusaku Miyata, MD; Rumi Maruyama, BS; Atsushi Mikami, MD, PhD; Shinya Minatoguchi, MD, PhD; Takako Fujiwara, MD, PhD; Hisayoshi Fujiwara, MD, PhD

Background—Fibrosis and progressive failure are prominent pathophysiological features of hearts after myocardial infarction (MI). We examined the effects of inhibiting transforming growth factor-β (TGF-β) signaling on post-MI cardiac fibrosis and ventricular remodeling and function.

Methods and Results—MI was induced in mice by left coronary artery ligation. An adenovirus harboring soluble TGF-β type II receptor (Ad.CAG-sTβRII), a competitive inhibitor of TGF-β, was then injected into the hindlimb muscles on day 3 after MI (control, Ad.CAG-LacZ). Post-MI survival was significantly improved among sTβRII-treated mice (96% versus control at 71%), which also showed a significant attenuation of ventricular dilatation and improved function 4 weeks after MI. At the same time, histological analysis showed reduced fibrous tissue formation. Although MI size did not differ in the 2 groups, MI thickness was greater and circumference was smaller in the sTβRII-treated group; within the infarcted area, α-smooth muscle actin–positive cells were abundant, which might have contributed to infarct contraction. Apoptosis among myofibroblasts in granulation tissue during the subacute stage (10 days after MI) was less frequent in the sTβRII-treated group, and sTβRII directly inhibited Fas-induced apoptosis in cultured myofibroblasts. Finally, treatment of MI-bearing mice with sTβRII was ineffective if started during the chronic stage (4 weeks after MI).

Conclusions—Postinfarction gene therapy aimed at suppressing TGF-β signaling mitigates cardiac remodeling by affecting cardiac fibrosis and infarct tissue dynamics (apoptosis inhibition and infarct contraction). This suggests that such therapy may represent a new approach to the treatment of post-MI heart failure, applicable during the subacute stage. ***(Circulation.* 2005;111:2430-2437.)**

Key Words: heart failure ■ gene therapy ■ myocardial infarction ■ transforming growth factors

Myocardial infarction (MI) often leads to left ventricular (LV) remodeling, which is characterized by ventricular dilatation, diminished cardiac performance, and poor recovery of function.[1] Thus, patients who escape death during the acute stage of a large MI are at high risk of developing heart failure during the chronic stage. Indeed, patients with postinfarction heart failure account for nearly half of the candidates for cardiac transplantation.[2] The extent of the cardiomyocyte death during the acute stage of MI is a critical determinant of the subsequent ventricular remodeling and eventual heart failure, but the complex process of cardiac remodeling is not determined solely by that; hypertrophic responses occur in cardiomyocytes in the surviving portion of the ventricle, followed by ventricular dilatation due to architectural rearrangement of the cardiomyocytes and interstitial cells making up the myocardium.[3–5] In that regard, myocardial fibrosis is one of the most characteristic structural changes in infarcted hearts and contributes to both systolic and diastolic dysfunction.[6,7]

See p 2416

Several lines of evidence point to the critical role played by transforming growth factor-β (TGF-β) during the progression of myocardial fibrosis: (1) TGF-β1 induces increases in both the production and secretion of collagen, increases the abundance of collagen type I and III mRNA in cultured rat cardiac fibroblasts, and stimulates the expression of extracellular matrix proteins in vivo[8]; (2) in vivo gene transfer of TGF-β1 can induce myocardial fibrosis[8]; (3) expression of TGF-β is markedly increased in both infarcted and noninfarcted areas

Received August 11, 2004; revision received January 4, 2005; accepted January 6, 2005.

From the Second Department of Internal Medicine (H.O., G.T., Y.L., M.E., S. Miyata, R.M., S. Minatoguchi, H.F.) and Department of Gene Therapy and Regenerative Medicine (K.K., T.T., K.Y., A.M.), Gifu University School of Medicine, Gifu; and Department of Food Science, Kyoto Women's University, Kyoto (T.F.), Japan.

Correspondence to Hisayoshi Fujiwara, MD, PhD, Second Department of Internal Medicine, Gifu University School of Medicine, 1-1 Yanagido, Gifu 501-1194, Japan. E-mail gifuim-gif@umin.ac.jp

Circulation **is available at http://www.circulationaha.org**

DOI: 10.1161/01.CIR.0000165066.71481.8E

of hearts after MI[9,10]; and (4) TGF-β is associated with angiotensin II–mediated fibrosis, whereas inhibition of angiotensin II signaling mitigates post-MI cardiac remodeling and improves function.[11,12] Collectively, these findings suggest strongly that TGF-β plays a critical role during the healing process after MI and thus affects cardiac remodeling and function during the chronic stage.

Soluble TGF-β type II receptor (sTβRII) inhibits the action of TGF-β, most likely by adsorbing TGF-β or by acting as a dominant negative receptor.[13] In the present study we hypothesized that postinfarction treatment with sTβRII would mitigate chronic heart failure by affecting the LV remodeling process. We therefore constructed a recombinant adenoviral vector expressing the extracellular domain of the TGF-β type II receptor fused to human immunoglobulin Fc and started its transduction into mouse hindlimbs (systemic transfection) on the third day after MI, a time when therapy would not affect acute ischemic death of cardiomyocytes. We then examined the effects on LV structure and function during the chronic stage of MI and sought possible mechanisms responsible for our observations made both in vitro and in vivo.

Methods

Replication-Defective Recombinant Adenoviral Vectors

A replication-defective adenoviral vector, Ad-TβRIIEx-Fc, which expresses the extracellular domain of the type II TGF-β receptor[13] fused to the Fc portion of human IgG1 under the transcriptional control of cytomegalovirus immediate early enhancer and a modified chicken β-actin promoter, was constructed by in vitro ligation as previously described.[14] Likewise, control Ad-LacZ was prepared as previously described.[15,16]

Measurement of sTβIIR in Plasma

Plasma concentrations of sTβRII after adenoviral transfection were measured in mice (n=5) by detecting human IgG-Fc with the use of an enzyme-linked immunosorbent assay (Institute of Immunology).

Experimental Protocols

The study was approved by our institutional animal research committee. MI was induced in 10-week-old male C57BL/6J mice (Chubu Kagaku, Nagoya, Japan) by ligating the left coronary artery as previously described.[14] In sham-operated mice, the suture was passed but not tied. Ad.CAG-sTβRII (1×10^{11} particles per mouse) was then injected into the hindlimb muscles of the mice. As a control, adenovirus harboring the LacZ gene (Ad.CMV-LacZ) was injected in the same manner.

Protocol 1 (Treatment at Subacute Stage)

MI was induced in 75 mice. Of those, 55 survived to the third day after MI and were entered into the study. They were then randomly assigned into sTβRII (n=27) and LacZ (n=28) treatment groups and were followed up for 4 weeks after MI. Fifteen sham-operated mice were subjected to either of the treatments (LacZ, n=7; sTβRII, n=8) and similarly assessed. In another experiment, on the third day after MI, 10 mice were divided into sTβRII and LacZ treatment groups (n=5 each), and the survivors (n=4 in the sTβRII group and n=3 in the LacZ group) were euthanized on day 10 after MI.

Protocol 2 (In Vitro Experiment)

MI was induced in mice, and 10 days later cardiac myofibroblasts were obtained from the infarcted areas of the hearts according to the method previously described with modification.[16] Briefly, the heart was resected, and the infarcted area was removed. The tissue was then minced and incubated with collagenase type II (Worthington) in Krebs-Ringer buffer for 30 minutes at 37°C. The dissociated cells were plated on 10-cm dishes for 1 hour and then rigorously washed with buffer. The attached remaining nonmyocytes were cultured in DMEM supplemented with 5% mouse serum, which was obtained from mice 7 days after transfection with Ad.CAG-TβRII or Ad.CMG-LacZ. The cells were used for experimentation during the second and third passages. More than 90% of the cells were found to be α-smooth muscle actin (SMA) positive. A mixture of agonistic anti-Fas antibody (1 μg/mL; Pharmingen) and actinomycin D (0.05 μg/mL; Sigma) was applied for 24 hours to induce apoptosis.[17]

Protocol 3 (Treatment at Chronic Stage)

MI was induced in 33 mice that were subsequently observed for 4 weeks with no treatment. At that time, scarring was well established in the infarcts of the 25 surviving mice, and gene treatment with LacZ (n=11) or sTβRII (n=14) was started. These mice were then examined after an additional 4 weeks (8 weeks after MI). In another set of animals, we evaluated sTβRII in the 5-week-old infarcted area (1 week after viral injection) by Western blot using LacZ gene– and sTβRII gene–treated hearts (n=3 each). This was to confirm accessibility of sTβRII into scar tissue.

Physiological Studies

Echocardiograms were recorded 4 weeks after MI with the use of an echocardiographic system (Aloka) equipped with a 7.5-MHz imaging transducer. The right carotid artery was then cannulated with a micromanometer-tipped catheter (SPR 407, Millar Instruments) that advanced into the left ventricle via the aorta for recording pressures and ±dP/dt.

Histological Analysis

After the physiological analyses, all surviving mice were euthanized, and their hearts were removed. The excised hearts were cut into 2 transverse slices; the basal specimens were fixed in 10% buffered formalin and embedded in paraffin, after which 4-μm-thick sections were stained with hematoxylin-eosin, Masson's trichrome, and Sirius red F3BA (0.1% solution in saturated aqueous picric acid) (Aldrich).[14] Quantitative assessments of cell size, cell population, and fibrotic area were performed on 20 randomly chosen high-power fields (HPF) in each section with the use of a LUZEX F multipurpose color image processor (Nireco). Quantitative assessments of cardiomyocyte size (as the transverse diameter), cell population, vessel population, and fibrotic area were performed on 20 randomly chosen HPF in each section with a LUZEX F multipurpose color image processor (Nireco). The number of cardiomyocytes evaluated was 198±12 cells per heart. Vessels were identified as the lumens outlined by Flk-1–positive endothelial cells on the Flk-1–immunostained sections.

Immunohistochemical Analysis

Deparaffinized 4-μm-thick sections or cultured cells were incubated with primary antibody against α-SMA (Sigma), Flk-1 (Santa Cruz), or pan-leukocyte antigen (CD45, Pharmingen), after which they were immunostained with diaminobenzidine hydrochloride or labeled with immunofluorescent Alexa Fluor 488 or 568 (Molecular Probes). Nuclei were stained with hematoxylin or Hoechst 33342.

Apoptosis was evaluated with the use of the in situ terminal deoxynucleotidyl transferase–mediated nick-end labeling (TUNEL) method with an ApopTag kit (Intergene) as previously described.[14]

For double immunofluorescence, tissue sections or cells were stained first with the use of an FITC-conjugated ApopTag kit (Integene) and then with anti–α-SMA or anti–Flk-1 followed by labeling with Alexa Fluor 568.

Western Blotting

Proteins (100 μg) extracted from hearts in protocol 1 were subjected to 14% polyacrylamide gel electrophoresis and then transferred onto polyvinylidene difluoride membranes. The membranes were then probed with the primary antibody against matrix metalloproteinase-2 (MMP-2) (Daiichi Fine Chemical Co) or atrial natriuretic peptide (ANP) (Santa Cruz).

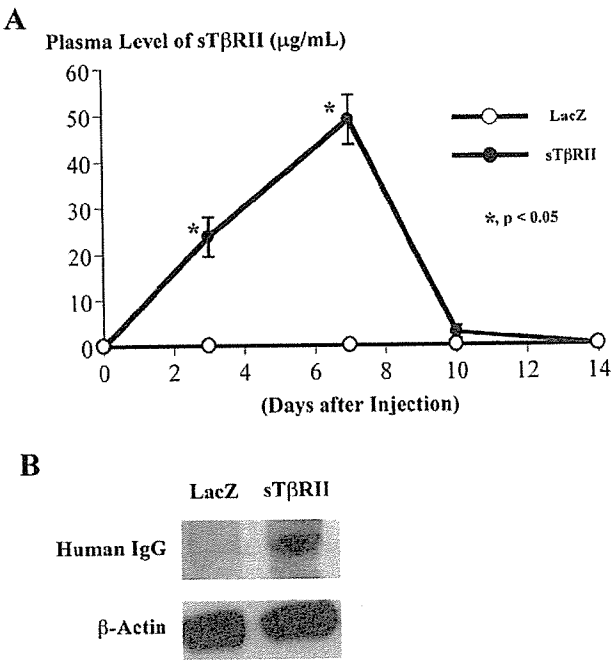

Figure 1. A, Time courses of changes in sTβRII levels measured by enzyme-linked immunosorbent assay in plasma from mice transfected with the LacZ or sTβRII gene. B, Expression of sTβRII protein in infarcted tissues as detected by anti-human IgG.

Infarct tissues were subjected to Western blotting for sTβRII by anti-human IgG antibody (DAKO).

The blots were visualized by means of chemiluminescence (ELC, Amersham), and the signals were quantified by densitometry. β-Actin (analyzed with antibody from Sigma) was the loading control.

Statistical Analysis

Values are shown as mean±SEM. Survival was analyzed by the Kaplan-Meier method with the log-rank Cox-Mantel method. The significance of differences was evaluated with Student *t* tests. Values of $P<0.05$ were considered significant.

Results

Plasma Levels of Exogenous sTβRII

Among mice receiving sTβRII gene transfection, the plasma levels of exogenous sTβRII reached 23.7±4.3 and 49.0±5.4 μg/mL, respectively, 3 and 7 days after the injection (6 and 10 days after MI, respectively), a time when the infarcted area was composed of granulation tissue (Figure 1A). Levels declined steeply thereafter, and sTβRII was undetectable in the plasma 2 weeks after MI. No sTβRII was detected in the LacZ-treated mice at any time. Accessibility of sTβRII into scar tissue was confirmed by Western blotting (Figure 1B). All sham-operated mice survived until 4 weeks after surgery.

Effect of Anti–TGF-β Treatment at Subacute Stage (Protocol 1)

Four Weeks After MI

The survival rate was significantly higher among sTβRII-treated mice than among LacZ-treated control mice 4 weeks after MI (Figure 2A): 26 of 27 mice (96%) in the sTβRII-

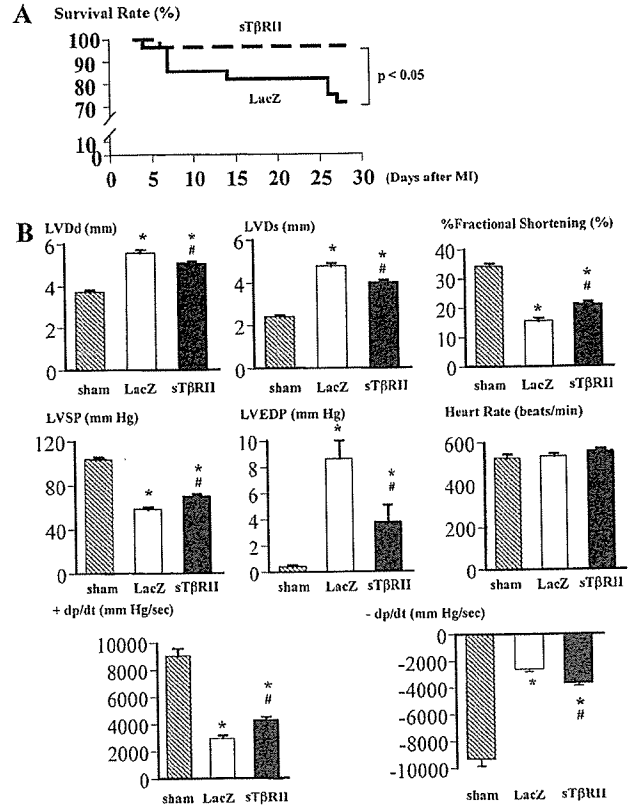

Figure 2. Survival, LV geometry, and LV function during the chronic stage (4 weeks after MI) in MI-bearing mice receiving gene therapy on day 3 after MI. A, Post-MI survival curves for LacZ-treated and sTβRII-treated mice. B to G, Effects of sTβRII therapy on cardiac anatomy and function 4 weeks after MI. LVDd and LVDs indicate left ventricular end-diastolic and end-systolic diameter, respectively; LVSP and LVEDP, left ventricular peak systolic and end-diastolic pressure, respectively; sham, sham-operated control group with LacZ gene treatment. *$P<0.05$, significant difference compared with sham; #$P<0.05$, significant difference compared with the LacZ-treated MI group.

treated group survived versus 20 of 28 mice (71%) in the control group ($P<0.05$).

Echocardiography and cardiac catheterization performed 4 weeks after MI showed control mice to have severe LV remodeling with marked enlargement of the LV cavity and signs of reduced cardiac function compared with the sham-operated mice (Figure 2B): decreased LV percent fractional shortening and ±dP/dt and increased LV end-diastolic pressure. These parameters were all attenuated in sTβRII-treated mice (Figure 2B), indicating mitigation of postinfarct remodeling and improved cardiac function. In the sham-operated mice, there was no significant difference in cardiac function 4 weeks after surgery between the sTβRII gene– and LacZ gene–treated group, indicating a negligible effect of sTβRII treatment on cardiac function of sham-operated mice (data not shown).

There was no significant difference in heart weights (Lac Z, 166±9 mg versus sTβRII, 168±6 mg) or in ratios of heart weight to body weight (Lac Z, 6±0.2 mg/g versus sTβRII, 6±0.3 mg/g) between the groups. Although hearts from LacZ-treated mice showed marked LV dilatation with a thin

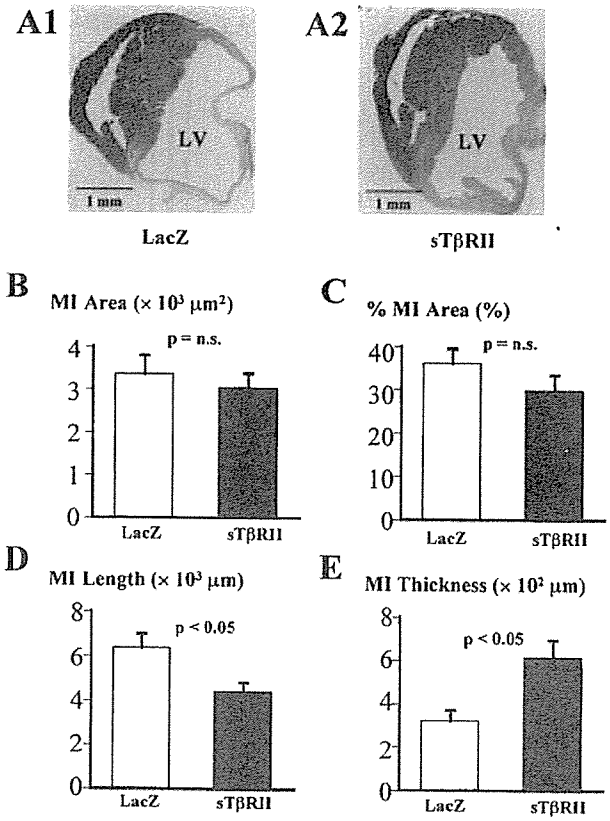

Figure 3. Morphometry of mouse hearts 4 weeks after MI. A, Transverse sections of hearts from mice treated with LacZ (A1) or sTβRII (A2). The sections are stained with Masson's trichrome. Note the smaller LV cavity, shorter infarct segment, and thicker infarct wall in the post-MI heart treated with sTβRII compared with the control heart. B, Absolute area of infarct. C, Percent area of left ventricle taken up by infarct. D, Thickness of infarct. E, Circumferential length of infarct segment.

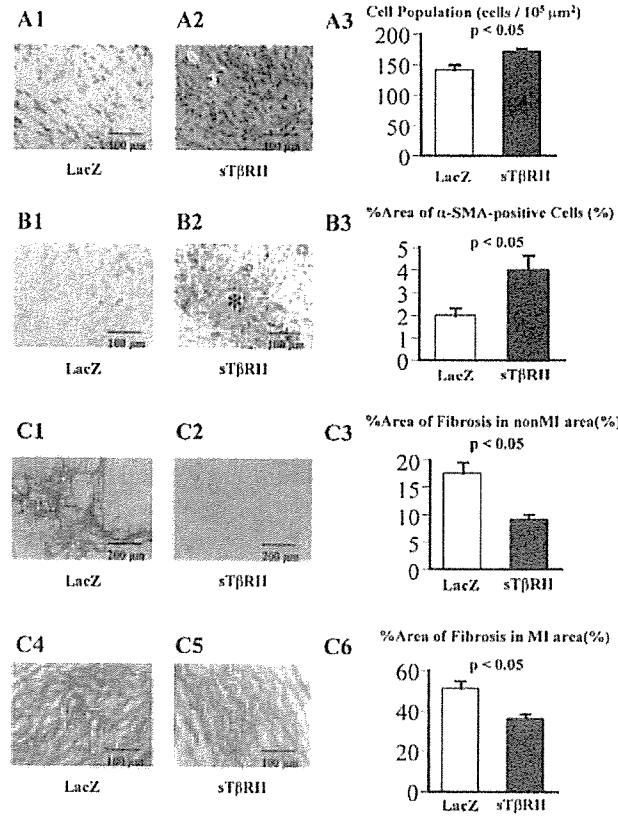

Figure 4. Histological and immunohistochemical preparations from mouse hearts collected 4 weeks after MI. A, Infarcted areas in hearts from LacZ-treated (A1) and sTβRII-treated (A2) mice; graph shows cell density (A3). Sections are stained with hematoxylin-eosin. B, Immunohistochemical analysis of α-SMA within infarcted areas of LacZ-treated (B1) and sTβRII-treated (B2) mice; graph shows percentage of infarcted area taken up by α-SMA–positive cells (B3). Asterisk in B2 indicates a bundle of α-SMA–positive cells. C, Sirius red–stained preparations of noninfarcted (C1 and C2) and infarcted (C4 and C5) areas in LacZ-treated (C1 and C4) and sTβRII-treated (C2 and C5) mice; graphs show percentage of noninfarcted (C3) and infarcted (C6) areas taken up by collagen fibers.

infarcted segment 4 weeks after MI, those from sTβRII-treated mice presented smaller LV cavities (Figure 3A1 and 3A2). Both the absolute area of the infarct and the percentage of the whole LV area taken up by the infarct were comparable between the LacZ- and sTβRII-treated mice (Figure 3B and 3C). On the other hand, the circumferential length of the infarcted segment was shorter and the infarct was thicker in the sTβRII-treated mice (Figure 3D and 3E).

By 4 weeks after MI, the infarcted areas of LacZ-treated mice had been replaced by fibrous scar tissue (Figure 4A1). The infarcts of sTβRII-treated mice, by contrast, contained not only collagen fibers but also numerous cells (Figure 4A2). The noncardiomyocyte population in the infarcted areas was significantly greater in the sTβRII-treated mice (Figure 4A3), as was the percent infarcted area taken up by extravascular α-SMA–positive cells (Figure 4B1 to 4B3). Some α-SMA–positive cells accumulated and formed bundles to run parallel with the infarct wall circumference (Figure 4B2) that were not observed in the infarcted LV walls of the control mice. Still, the population of vessels was comparable in the 2 groups (LacZ, 7.2±0.7 vessels per HPF versus sTβRII, 6.9±0.8 vessels per HPF; P=NS). There was no significant difference in population of CD45-positive cells between the control (0.9±0.1 cells per HPF) and sTβRII-treated hearts (0.8±0.2 cells per HPF; P=NS). The amount of fibrosis assessed in Sirius red–stained sections was significantly reduced in the noninfarcted LV walls and in the infarct region of the sTβRII-treated mice (Figure 4C1 to 4C6). MMP-2 in hearts with 4-week-old MI was greater in hearts with MI compared with the sham-operated hearts, but it was not significantly affected by the sTβRII treatment (Figure 5A and 5B), suggesting a negligible association of the gelatinase activity with sTβRII-induced antifibrosis in the present experimental setting. In addition, the transverse diameters of cardiomyocytes in the noninfarcted areas were significantly greater in the LacZ-treated (17.7±0.3 μm) than in the sTβRII-treated (15.1±0.3 μm) mice (Figure 5C), suggesting that the compensatory cardiomyocyte hypertrophy was more developed in the control mice. Consistent with this finding, Western blot analysis revealed reduced ANP expression in the sTβRII-treated hearts (Figure 5A and 5B).

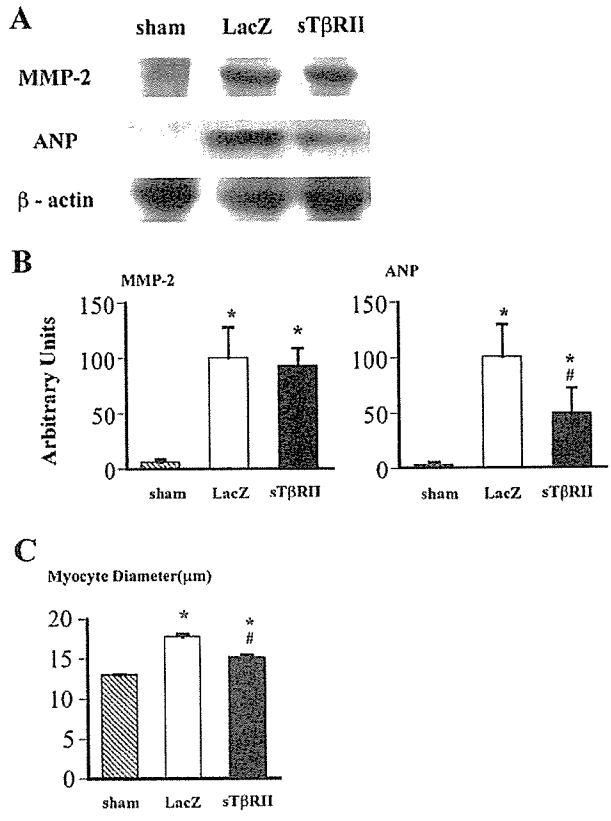

Figure 5. A, Western blotting for MMP-2 and ANP of sham-operated heart and hearts with 4-week-old MI. B, Densitometry of MMP-2 (left) and ANP (right). C, Cardiomyocyte size in sham-operated control hearts and hearts with 4-week-old MI. *$P<0.05$, significant difference compared with sham; #$P<0.05$, significant difference compared with the LacZ-treated MI group.

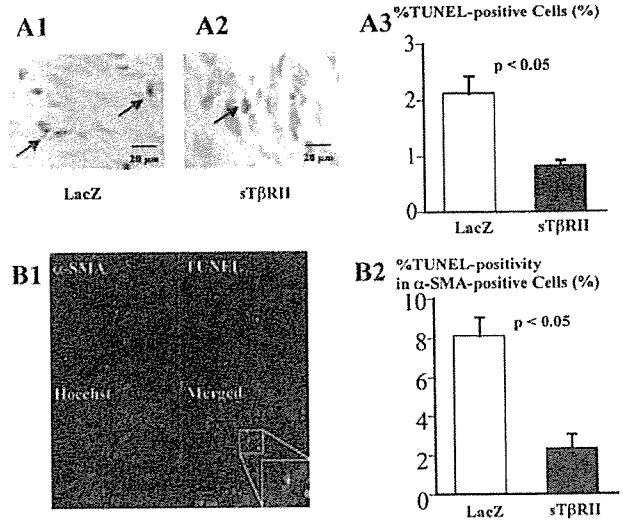

Figure 6. Apoptosis within infarcted tissue 10 days after MI. A, TUNEL-stained preparations from LacZ-treated (A1) and sTβRII-treated (A2) mice. A3, Percentage of TUNEL-positive nonmyocytes within the infarcted area. Arrows indicate positive cells. B, Infarcted tissue obtained from LacZ-treated mice (B1) was double stained with TUNEL and α-SMA immunohistochemistry and observed under a confocal microscope. B2, Percentage of TUNEL-positive cells among the α-SMA–positive cells.

Ten Days After MI

By 10 days after MI, the infarcted areas were composed of granulation tissue, and TUNEL assays indicated that apoptosis was ongoing in both the LacZ- and sTβRII-treated groups. However, the incidence of TUNEL-positive cells was significantly smaller in the sTβRII-treated than in the LacZ-treated group (Figure 6A1 to 6A3). Moreover, double-immunofluorescence assays (TUNEL followed by anti–Flk-1 or anti–SMA antibody) revealed that within the sTβRII-treated group, the incidence of apoptosis was reduced among myofibroblasts/smooth muscle cells (Figure 6B1 and 6B2) but not among endothelial cells (LacZ, 3.5±0.5% versus sTβRII, 3.5±0.2%; P=NS), which suggests that sTβRII may specifically inhibit apoptosis among myofibroblasts. TUNEL-positive cardiomyocytes were extremely rare (<0.01%) in both groups.

Effect of sTβRII on Fas-Induced Apoptosis In Vitro (Protocol 2)

Myofibroblasts obtained from the infarcted areas of mouse hearts 10 days after MI were cultured in medium containing 5% serum collected from LacZ- or sTβRII-treated mice. When the cells were then subjected to Fas-induced apoptosis[16] for 24 hours, the incidence of TUNEL-positive myofibroblasts was significantly lower among cells cultured with sTβRII-containing serum (16±2.9%) than among those cultured with normal serum (43±5.2%; $P<0.05$) (Figure 7). However, such an apoptosis-inhibitory effect by sTβRII-containing serum was completely canceled by an addition of TGF-β1 at the concentration of 1 μg/mL (Figure 7). These findings suggest that sTβRII exerts a direct antiapoptotic effect on cardiac myofibroblasts.

Effect of Anti–TGF-β Treatment at Chronic Stage (Protocol 3)

Using protocol 3, we determined the extent to which inhibiting apoptosis among granulation tissue cells is responsible for the beneficial effects on post-MI heart failure. For this purpose, the sTβRII gene therapy was started at a more chronic stage of MI, after the granulation tissue had already been replaced with scar tissue. The sTβRII (n=14) or LacZ (n=11) gene was delivered to mice 4 weeks after MI, and the mice were examined after an additional 4 weeks (8 weeks after MI). Accessibility of sTβRII into scar tissue was confirmed by Western blotting (Figure 1B). One of 14 sTβRII-treated mice and none of the 11 LacZ-treated mice died during the additional 4-week follow-up (P=NS). This time we found no difference in ventricular geometry or function between the sTβRII-treated and LacZ-treated groups (Table), clearly indicating that the preventive effect of sTβRII gene therapy on heart failure is attributable to its action on granulation tissue during the subacute stage of MI.

Discussion

The present study revealed that postinfarction sTβRII gene therapy, begun at the subacute stage of MI, alleviated adverse remodeling and improved function of the LV during the chronic stage. In addition, we provide novel insights into the

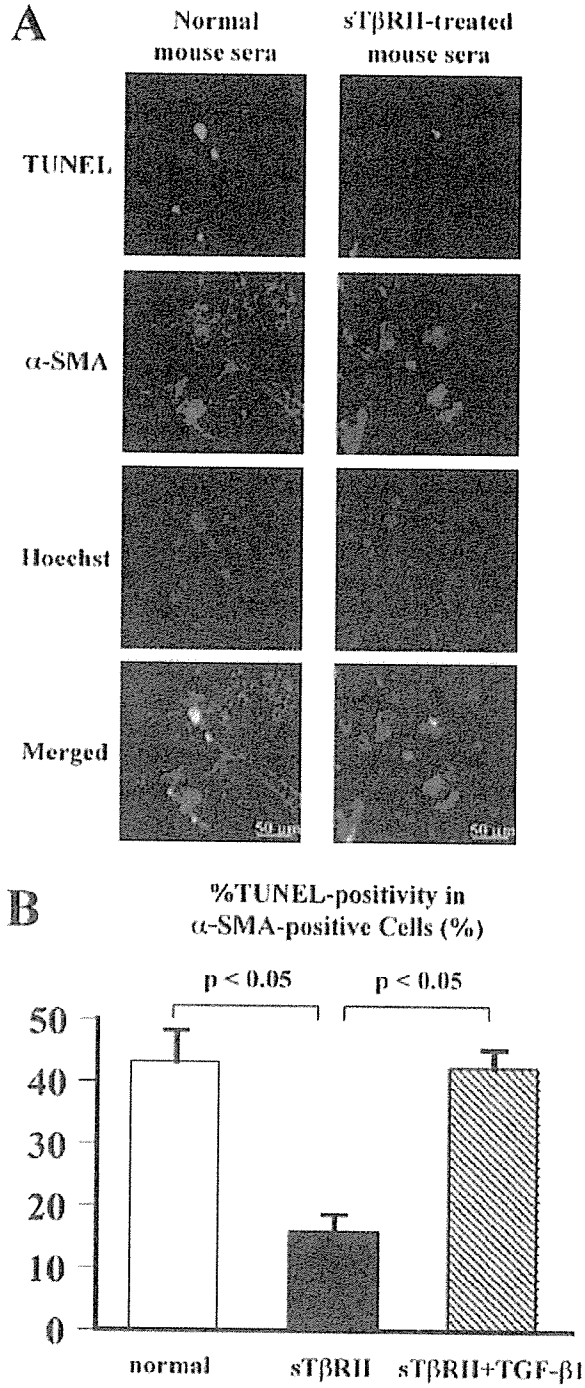

Figure 7. Effect of sTβRII-containing sera on Fas-induced apoptosis among cultured nonmyocytes obtained from the infarcted tissue of hearts 10 days after MI (protocol 2). Confocal micrographs (A) show TUNEL-positive/α-SMA-positive cultured cells. B, Percentage of apoptotic myofibroblasts.

mechanism of the beneficial effect of the TGF-β signal inhibition.

Mechanisms of Beneficial Effects of sTβRII on Postinfarction Heart Failure

The mechanisms responsible for the beneficial effects of inhibiting TGF-β signaling on post-MI heart failure appear somewhat complicated, probably reflecting the multiple biological effects of TGF-β. TGF-β signaling acts as a strong inducer of extracellular matrix and as an immunomodulator of chemotaxis by fibroblasts and inflammatory cells.[18–20] In the infarcted heart, TGF-β expression is regulated by locally generated angiotensin II via angiotensin II type 1 receptor binding, and angiotensin-converting enzyme inhibitors and angiotensin II type 1 receptor blockade attenuated postinfarction ventricular remodeling equally.[11,12] However, the manner in which direct inhibition of TGF-β signaling in the infarcted heart affects the postinfarction process has not been well elucidated . In the present study inhibition of TGF-β signaling by exogenous sTβRII significantly reduced cardiac fibrosis, confirming the fibrogenetic effect of TGF-β on post-MI hearts. Because myocardial fibrosis contributes to both systolic and diastolic dysfunction in the heart,[6,7] reducing it by inhibiting TGF-β signaling is one way in which to mitigate LV remodeling and heart failure. MMP-2 activity seemed to be not significantly associated with sTβRII-induced antifibrosis in the present experimental setting.

Perhaps the most notable finding of the present study is the effect of anti–TGF-β therapy on infarct geometry, ie, the shortening of the infarcted segment and the thickening of the infarcted wall, without a change in absolute infarcted area. Contraction of the infarcted tissue likely contributes to suppression of LV dilatation. Because wall stress is proportional to the cavity diameter and inversely proportional to the wall thickness (Laplace's law)[21] and because wall stress and adverse LV remodeling (dilatation) have a vicious relationship, accelerating one another, it is easy to surmise that such an alteration in the geometry of the infarct would markedly improve the hemodynamic state of the heart.

Ventricular Geometry, Function, and Histology 8 Weeks After MI Among Mice Transfected With the Indicated Gene 4 Weeks After MI (Protocol 3)

	LacZ (n=11)	sTβRII (n=13)	P
LVED diameter, mm	6.0±0.1	6.3±0.2	0.11
% Fractional shortening	16.7±0.6	16.1±0.6	0.53
Heart rate, bpm	502±21	544±20	0.16
LVSP, mm Hg	85±3	80±3	0.21
LVEDP, mm Hg	9±1	9±1	0.84
+dP/dt, mm Hg/s	3847±101	3608±150	0.22
−dP/dt, mm Hg/s	−3642±166	−3337±144	0.18
MI area, $\times 10^3$ μm^2	2.1±0.2	2.4±0.3	0.53
% MI area	21.5±3.2	24.2±3.0	0.57
MI segmental length, $\times 10^3$ μm	6.1±0.9	6.4±0.7	0.78
MI wall thickness, $\times 10^2$ μm	2.4±0.4	2.0±0.2	0.43
% Fibrosis in non-MI area	17.7±1.8	18.1±1.9	0.88
% Fibrosis in MI area	50.6±3.6	51.5±3.9	0.56
Cell population in MI area, cells/10^5 μm^2	149±6	144±5	0.56
Area of α-SMA–positive cells, %	1.9±0.9	2.0±0.2	0.75

LVED indicates LV end-diastolic; LVSP, LV peak systolic pressure; and LVEDP, LV end-diastolic pressure.

Inhibition of TGF-β signaling also qualitatively altered the infarct tissue. We found an increased abundance of α-SMA–positive cells (myofibroblasts and smooth muscle cells) in the extravascular area of infarcts in sTβRII-treated hearts. Those cells are well known to play an important role in wound contraction during the healing process,[22] and to then disappear via apoptosis.[23,24] Recently, we reported that blockade of myofibroblast apoptosis by the treatment with pan-caspase inhibitor or with soluble Fas, a competitive inhibitor of Fas, attenuates postinfarction ventricular remodeling and heart failure.[25,26] We speculate that the preserved myofibroblasts may contribute structurally to the thickening of the infarct scar. In addition, although the property of contractile function of these myofibroblasts has not been elucidated, it is conceivable that contractile myofibroblasts that are running parallel with the infarct circumference may shrink the infarct into coronal directions and increase the infarct thickness.

It is thus notable that sTβRII had a direct inhibitory effect on apoptosis among myofibroblasts in granulation tissue, both in vivo and in vitro. This is consistent with the report by Hagimoto et al,[27] who showed that TGF-β1 sensitizes pulmonary epithelial cells to Fas-induced apoptosis. Conversely, TGF-β is known to promote transdifferentiation of fibroblasts into myofibroblasts,[28] ie, inhibition of TGF-β signaling possibly results in reduction of myofibroblast population. Inhibition of TGF-β signaling thus appears to have reciprocal effects on myofibroblast population: its reduction through interfering with transdifferentiation from fibroblasts and its augmentation through blocking apoptotic death. In the present experimental setting, the gene product peaked during the granulation tissue phase (1-week-old infarct) when myofibroblasts were already abundant but their apoptosis was ongoing. In the 4-week-old infarct tissue, however, naturally occurring apoptosis was already complete in the control MI hearts. These findings may explain our data that the population of α-SMA–positive cells was balanced to gain in the post-MI scar tissue of the TGF-β signal–inhibited hearts. Taken together, these findings suggest that myofibroblasts escaping apoptosis may survive even during the chronic stage of MI, accumulate, form bundles, and contribute to infarct contraction. In addition, this mechanism appears critical for functional improvement, as transfection of the sTβRII gene was ineffective if started during the chronic stage of MI, when most α-SMA–positive cells have already disappeared (see protocol 3 above).

Because in the present study sTβRII gene therapy was started on the third day after MI, it is unlikely that it influenced cardiomyocyte apoptosis during the acute stage. It is also unlikely that this therapy affected cardiomyocyte survival by inhibiting apoptosis at the subacute or chronic stages. This is because, in contrast to an earlier report,[4] we found that apoptosis was negligible among cardiomyocytes at any stage of MI.

Time Window Within Which to Inhibit TGF-β Signaling

TGF-β signaling is believed to have cardioprotective effect during ischemia/reperfusion, perhaps as a result of inhibition of tumor necrosis factor-α release, improvement of endothelium-dependent relaxation, prevention of reactive oxygen species generation, and/or inhibition of upregulation of matrix metalloproteinase-1.[29,30] For these reasons, inhibition of TGF-β signaling during the acute stage of MI is considered harmful. In addition, our data indicate that late inhibition of TGF-β signaling (during the scar phase of MI) is without effect. It thus appears that there is a therapeutic time window that is critical for inhibition of TGF-β signaling to elicit the beneficial effects on post-MI heart failure.

Limitations and Clinical Implications

There is considerable evidence indicating that the TGF-β signal exerts a protective effect against atherosclerosis in mouse models by preventing lipid lesion formation.[31–33] This potential limitation might have to be taken into account in application of the anti–TGF-β strategy.

Rapid recanalization of the occluded coronary artery is presently the best clinical approach to the treatment of acute MI; if performed in time, it enables salvage of the ischemic myocardial cells. Unfortunately, most patients miss the chance for coronary reperfusion therapy because to be effective it must be performed within a few hours after the onset of infarction.[34] The present findings suggest that this novel therapeutic strategy may mitigate the chronic progressive heart failure seen in patients after large MIs. When initiated during the subacute stage, inhibition of TGF-β signaling may benefit patients who missed the chance for coronary reperfusion.

Acknowledgments

We thank Akiko Tsujimoto and Hatsue Ohshika for technical assistance.

References

1. Pfeffer MA, Braunwald E. Ventricular remodeling after myocardial infarction: experimental observations and clinical implications. *Circulation.* 1990;81:1161–1172.
2. Hosenpud JD, Bennett LE, Keck BM, Boucek MM, Novick RJ. The Registry of the International Society for Heart and Lung Transplantation: seventeenth official report: 2000. *J Heart Lung Transplant.* 2000;19:909–931.
3. Pfeffer JM, Pfeffer MA, Fletcher PJ, Braunwald E. Progressive ventricular remodeling in rat with myocardial infarction. *Am J Physiol.* 1991;260:H1406–H1414.
4. Cheng W, Kajstura J, Nitahara JA, Li B, Reiss K, Liu Y, Clark WA, Krajewski S, Reed JC, Olivetti G, Anversa P. Programmed myocyte cell death affects the viable myocardium after infarction in rats. *Exp Cell Res.* 1996;226:316–327.
5. Weisman HF, Bush DE, Mannisi JA, Weisfeldt ML, Healy B. Cellular mechanisms of myocardial infarct expansion. *Circulation.* 1988;78:186–201.
6. Burlew BS, Weber KT. Connective tissue and the heart: functional significance and regulatory mechanisms. *Cardiol Clin.* 2000;18:435–442.
7. Jalil JE, Doering CW, Janicki JS, Pick R, Shroff SG, Weber KT. Fibrillar collagen and myocardial stiffness in the intact hypertrophied rat left ventricle. *Circ Res.* 1989;64:1041–1050.
8. Lijnen PJ, Petrov VV, Fagard RH. Induction of cardiac fibrosis by transforming growth factor-beta1. *Mol Genet Metab.* 2000;71:418–435.
9. Hao J, Ju H, Zhao S, Junaid A, Scammell-La Fleur T, Dixon IM. Elevation of expression of Smad2, 3, and 4, decorin and TGF-beta in the chronic phase of myocardial infarct scar healing. *J Mol Cell Cardiol.* 1999;31:667–678.
10. Deten A, Holzl A, Leicht M, Barth W, Zimmer HG. Changes in extracellular matrix and in transforming growth factor beta isoforms after coronary artery ligation in rats. *J Mol Cell Cardiol.* 2001;33:1191–1207.
11. Schieffer B, Wirger A, Meybrunn M, Seitz S, Holtz J, Riede UN, Drexler H. Comparative effects of chronic angiotensin-converting enzyme inhi-

bition and angiotensin II type 1 receptor blockade on cardiac remodeling after myocardial infarction in the rat. *Circulation.* 1994;89:2273–2282.
12. Yu CM, Tipoe GL, Wing-Hon Lai K, Lau CP. Effects of combination of angiotensin-converting enzyme inhibitor and angiotensin receptor antagonist on inflammatory cellular infiltration and myocardial interstitial fibrosis after acute myocardial infarction. *J Am Coll Cardiol.* 2001;38: 1207–1215.
13. Isaka Y, Akagi Y, Ando Y, Tsujie M, Sudo T, Ohno N, Border WA, Noble NA, Kaneda Y, Hori M, Imai E. Gene therapy by transforming growth factor-beta receptor-IgG Fc chimera suppressed extracellular matrix accumulation in experimental glomerulonephritis. *Kidney Int.* 1999;55:465–475.
14. Li Y, Takemura G, Kosai K, Yuge K, Nagano S, Esaki M, Goto K, Takahashi T, Hayakawa K, Koda M, Kawase Y, Maruyama R, Okada H, Minatoguchi S, Mizuguchi H, Fujiwara T, Fujiwara H. Postinfarction treatment with an adenoviral vector expressing hepatocyte growth factor relieves chronic left ventricular remodeling and dysfunction in mice. *Circulation.* 2003;107:2499–2506.
15. Chen SH, Chen XH, Wang Y, Kosai K, Finegold MJ, Rich SS, Woo SL. Combination gene therapy for liver metastasis of colon carcinoma in vivo. *Proc Natl Acad Sci U S A.* 1995;92:2577–2581.
16. Katwa LC, Campbell SE, Tyagi SC, Lee SJ, Cicila GT, Weber KT. Cultured myofibroblasts generate angiotensin peptides de novo. *J Mol Cell Cardiol.* 1997;29:1375–1386.
17. Ni R, Tomita Y, Matsuda K, Ichihara A, Ishimura K, Ogasawara J, Nagata S. Fas-mediated apoptosis in primary cultured mouse hepatocytes. *Exp Cell Res.* 1994;215:332–337.
18. Moses HL, Yang EY, Pietenpol JA. TGF-beta stimulation and inhibition of cell proliferation: new mechanistic insights. *Cell.* 1990;63:245–247.
19. Postlethwaite AE, Keski-Oja J, Moses HL, Kang AH. Stimulation of the chemotactic migration of human fibroblasts by transforming growth factor beta. *J Exp Med.* 1987;165:251–256.
20. Lu L, Chen SS, Zhang JQ, Ramires FJ, Sun Y. Activation of nuclear factor-kappaB and its proinflammatory mediator cascade in the infarcted rat heart. *Biochem Biophys Res Commun.* 2004;321:879–885.
21. Yin FC. Ventricular wall stress. *Circ Res.* 1981;49:829–842.
22. Gabbiani G. The myofibroblast in wound healing and fibrocontractive diseases. *J Pathol.* 2003;200:500–503.
23. Desmouliere A, Redard M, Darby I, Gabbiani G. Apoptosis mediates the decrease in cellularity during the transition between granulation tissue and scar. *Am J Pathol.* 1995;146:56–66.
24. Takemura G, Ohno M, Hayakawa Y, Misao J, Kanoh M, Ohno A, Uno Y, Minatoguchi S, Fujiwara T, Fujiwara H. Role of apoptosis in the disappearance of infiltrated and proliferated interstitial cells after myocardial infarction. *Circ Res.* 1998;82:1130–1138.
25. Hayakawa K, Takemura G, Kanoh M, Li Y, Koda M, Kawase Y, Maruyama R, Okada H, Minatoguchi S, Fujiwara T, Fujiwara H. Inhibition of granulation tissue cell apoptosis during the subacute stage of myocardial infarction improves cardiac remodeling and dysfunction at the chronic stage. *Circulation.* 2003;108:104–109.
26. Li Y, Takemura G, Kosai K, Takahashi T, Okada H, Miyata S, Yuge K, Nagano S, Esaki M, Khai NC, Goto K, Mikami A, Maruyama R, Minatoguchi S, Fujiwara T, Fujiwara H. Critical roles for the Fas/Fas ligand system in postinfarction ventricular remodeling and heart failure. *Circ Res.* 2004;95:627–636.
27. Hagimoto N, Kuwano K, Inoshima I, Yoshimi M, Nakamura N, Fujita M, Maeyama T, Hara N. TGF-beta 1 as an enhancer of Fas-mediated apoptosis of lung epithelial cells. *J Immunol.* 2002;168:6470–6478.
28. Desmouliere A, Geinoz A, Gabbiani F, Gabbiani G. Transforming growth factor-beta 1 induces alpha-smooth muscle actin expression in granulation tissue myofibroblasts and in quiescent and growing cultured fibroblasts. *J Cell Biol.* 1993;122:103–111.
29. Lefer AM, Ma XL, Weyrich AS, Scalia R. Mechanism of the cardioprotective effect of transforming growth factor beta 1 in feline myocardial ischemia and reperfusion. *Proc Natl Acad Sci U S A.* 1993;90: 1018–1022.
30. Chen H, Li D, Saldeen T, Mehta JL. TGF-beta 1 attenuates myocardial ischemia-reperfusion injury via inhibition of upregulation of MMP-1. *Am J Physiol.* 2003;284:H1612–H1617.
31. Grainger DJ. Transforming growth factor beta and atherosclerosis: so far, so good for the protective cytokine hypothesis. *Arterioscler Thromb Vasc Biol.* 2004;24:399–404.
32. Mallat Z, Gojova A, Marchiol-Fournigault C, Esposito B, Kamate C, Merval R, Fradelizi D, Tedgui A. Inhibition of transforming growth factor-beta signaling accelerates atherosclerosis and induces an unstable plaque phenotype in mice. *Circ Res.* 2001;89:930–934.
33. Robertson AK, Rudling M, Zhou X, Gorelik L, Flavell RA, Hansson GK. Disruption of TGF-β signaling in T cells accelerates atherosclerosis. *J Clin Invest.* 2003;112:1342–1350.
34. Reimer KA, Vander Heide RS, Richard VJ. Reperfusion in acute myocardial infarction: effect of timing and modulating factors in experimental models. *Am J Cardiol.* 1993;72:13G–21G.

Critical Roles for the Fas/Fas Ligand System in Postinfarction Ventricular Remodeling and Heart Failure

Yiwen Li, Genzou Takemura, Ken-ichiro Kosai, Tomoyuki Takahashi, Hideshi Okada, Shusaku Miyata, Kentaro Yuge, Satoshi Nagano, Masayasu Esaki, Ngin Cin Khai, Kazuko Goto, Atsushi Mikami, Rumi Maruyama, Shinya Minatoguchi, Takako Fujiwara, Hisayoshi Fujiwara

Abstract—In myocardial infarction (MI), granulation tissue cells disappear via apoptosis to complete a final scarring with scanty cells. Blockade of this apoptosis was reported to improve post-MI ventricular remodeling and heart failure. However, the molecular biological mechanisms for the apoptosis are unknown. Fas and Fas ligand were overexpressed in the granulation tissue at the subacute stage of MI (1 week after MI) in mice, where apoptosis frequently occurred. In mice lacking functioning Fas (*lpr* strain) and in those lacking Fas ligand (*gld* strain), apoptotic rate of granulation tissue cells was significantly fewer compared with that of genetically controlled mice, and post-MI ventricular remodeling and dysfunction were greatly attenuated. Mice were transfected with adenovirus encoding soluble Fas (sFas), a competitive inhibitor of Fas ligand, on the third day of MI. The treatment resulted in suppression of granulation tissue cell apoptosis and produced a thick, cell-rich infarct scar containing rich vessels and bundles of smooth muscle cells with a contractile phenotype at the chronic stage (4 weeks after MI). This accompanied not only alleviation of heart failure but also survival improvement. However, the sFas gene delivery during scar tissue phase was ineffective, suggesting that beneficial effects of the sFas gene therapy owes to inhibition of granulation tissue cell apoptosis. The Fas/Fas ligand interaction plays a critical role for granulation tissue cell apoptosis after MI. Blockade of this apoptosis by interfering with the Fas/Fas ligand interaction may become one of the therapeutic strategies against chronic heart failure after large MI. **(*Circ Res.* 2004;95:627-636.)**

Key Words: apoptosis ■ gene therapy ■ heart failure ■ myocardial infarction ■ remodeling

Large myocardial infarction (MI) causes severe chronic heart failure with unfavorable remodeling of the left ventricle (LV), which is characterized by a ventricular dilatation and diminished cardiac performance.[1] The magnitude of acute MI, which is determined within several hours after an attack of MI,[2] is the most critical determinant of subsequent heart failure. However, many other factors, such as late death or hypertrophy of cardiomyocytes, fibrosis, and the expression of various cytokines, are associated with the disease progression.[3–6] Cardiomyocyte death resulting from apoptosis during chronic heart failure may play an important role in the disease progression,[7–9] although its role is still unclear because of a low incidence.[10–13] In contrast, nonmyocytes in the infarct area, such as infiltrating inflammatory cells during the acute stage and granulation tissue cells during the subacute stage of MI, do die via apoptosis as we reported previously.[14] Granulation tissue in particular contains an abundance of neovasculature, myofibroblasts, and macrophages. We reported recently that inhibition of granulation tissue cell apoptosis by use of Boc-Asp-fmk, a pancaspase inhibitor, significantly improved LV remodeling and heart failure at the chronic stage of MI.[15] However, the molecular mechanisms of this apoptosis have not been determined, although a dependency on caspases is recognized.

Fas/Fas ligand interaction is an important trigger for apoptosis in many cell types, particularly cells related to the immune system.[16] Because MI ensues inflammation and post-MI granulation tissue contains chronic inflammatory cells, we hypothesize that the Fas/Fas ligand system is involved in the apoptosis of granulation tissue cells. In the present study, we first report that the Fas/Fas ligand system is activated in post-MI granulation tissue cells and significantly influences the postinfarct process. Next, we show that inhibition of the Fas/Fas ligand system by delivery of the gene for soluble Fas, a competitive inhibitor of Fas/Fas ligand interaction,[17] during the subacute stage of MI could potentially prevent post-MI heart failure at the chronic stage.

Methods

Experimental MI in Mice

The study was approved by our institutional animal research committee. MI was created in male C57BL/6J wild-type mice and

Original received March 19, 2004; revision received July 7, 2004; accepted July 27, 2004.

From the Second Department of Internal Medicine (Y.L., G.T., H.O., S. Miyata, M.E., R.M., S. Minatoguchi, H.F.) and the Department of Gene Therapy and Regenerative Medicine (K.-i.K., T.T., K.Y., S.N., M.E., N.C.K., K.G., A.M.), Gifu University School of Medicine, Gifu; and the Department of Food Science (T.F.), Kyoto Women's University, Kyoto, Japan.

Correspondence to Hisayoshi Fujiwara, MD, PhD, Second Department of Internal Medicine, Gifu University School of Medicine, 1-1 Yanagido, Gifu 502-1194 Japan. E-mail gifuim-gif@umin.ac.jp

Circulation Research is available at http://www.circresaha.org

DOI: 10.1161/01.RES.0000141528.54850.bd

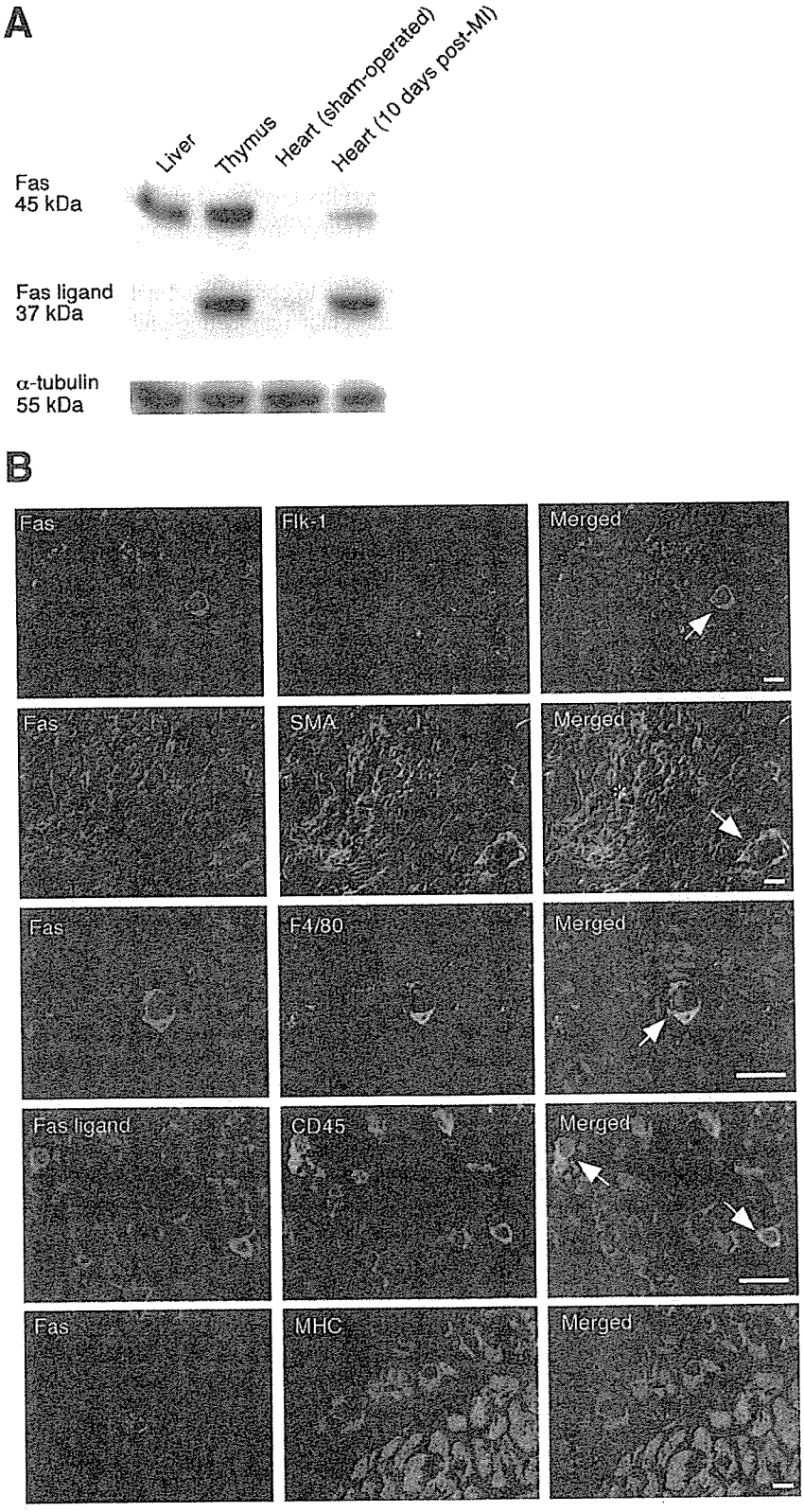

Figure 1. Augmented expression of Fas and Fas ligand in the infarct area 10 days after MI. A, Western blots for Fas and Fas ligand in normal liver, normal thymus, sham-operated heart, and heart with 10-day-old MI. Expression of both Fas and Fas ligand was significantly augmented in the heart with MI compared with the sham-operated heart. α-tubulin was a loading control. B, Double immunofluorescence for Fas or Fas ligand (red) combined with Flk-1, α-SMA, F4/80, CD34, or cardiac myosin heavy chain (MHC; green), under a confocal microscope. Fas positivity was seen in endothelial cells, vascular smooth muscle cells, extravascular myofibroblasts (asterisk), macrophages, and leukocytes but not in cardiomyocytes, whereas Fas ligand positivity was limited to leukocytes. Arrows and an asterisk indicate double-positive cells. Bars=20 μm.

syngenetic *lpr* mice and *gld* mice (Clea Japan; Shizuoka, Japan) at 12 weeks of age by ligating the left coronary artery as described.[18] In sham-operated mice, the suture was passed but not tied. Animals were killed 2 days, 10 days, 4 weeks, or 10 weeks after surgery.

Recombinant Adenoviral Vectors

Replication-incompetent adenoviral vector that ubiquitously and strongly expresses a chimeric fusion protein of exracellular region of mouse Fas and the Fc region of human IgG_1 (mFas-Fc), that is,

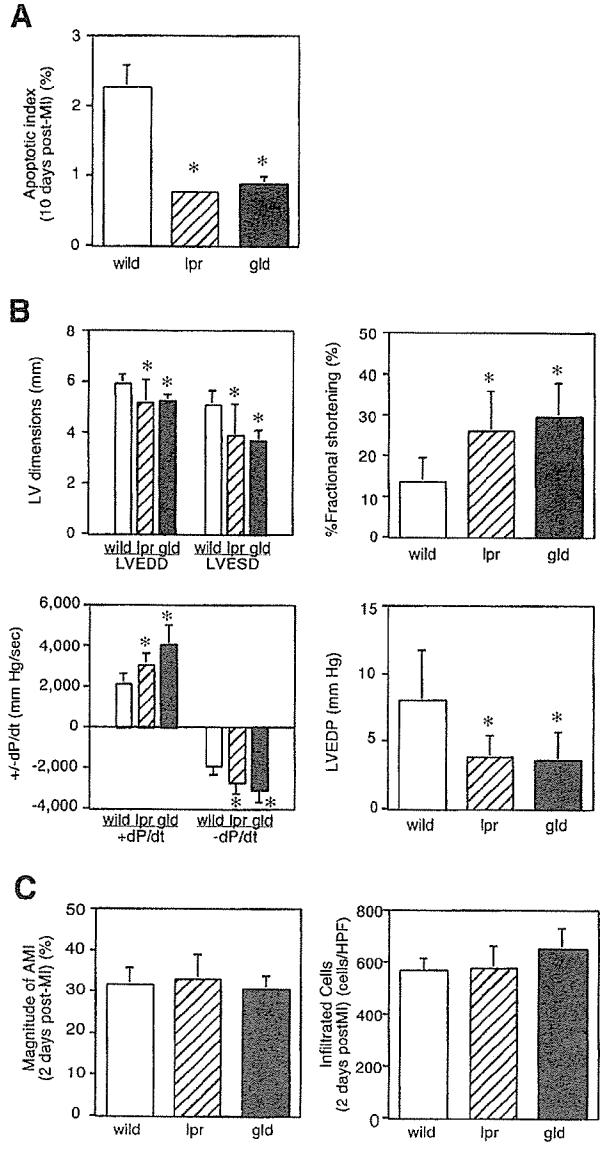

Figure 2. Modified post-MI ventricular remodeling and dysfunction in *lpr* and *gld* mice. A, Apoptotic index on the basis of a TUNEL assay in granulation tissue 10 days after MI in wild-type, *lpr*, and *gld* mice. *$P<0.05$ compared with wild-type. B, Anatomical and hemodynamic data for the hearts with a 4-week-old MI obtained from echocardiography and cardiac catheterization. *$P<0.05$ compared with wild-type mice. LVEDD indicates LV end-diastolic dimension; LVESD, LV end-systolic dimension. C, Magnitude of acute myocardial infarct (2-day-old MI) evaluated as the percentage of infarct area to total LV area in wild-type, *lpr*, and *gld* mice.

soluble Fas (sFas), was generated as follows. Adenoviral vector plasmid pAd-sFas, which comprises the cytomegalovirus immediate early enhancer, a modified chicken β-actin promoter and the extracellular region of mouse Fas (sFas) cDNA (Ad.CAG-sFas) was constructed by the in vitro ligation method (gift from Dr Mark A. Kay, Stanford University School of Medicine, California) as described previously.[19] Plasmid pFAS-FcII was generously provided by Dr S. Nagata (Osaka University Graduate School of Medicine, Japan).[20] Control Ad-LacZ was prepared as reported previously.[21]

On day 3 of MI, the sFas gene or LacZ gene was systemically delivered to mice by injection of Ad.CAG-sFas or Ad-LacZ (1×10^9 plaque-forming units[pfu]/mouse) into the hindlimb muscles.

Measurement of the sFas Level in Plasma

The plasma concentration of sFas was measured by detecting human IgG-Fc using an ELISA kit (Institute of Immunology).

Physiological Studies

Echocardiograms were recorded with an echocardiographic system (Aloka) equipped with a 7.5-MHz imaging transducer at 4 or 10 weeks after MI. After cardiac echocardiography, the right carotid artery was cannulated with a micromanometer-tipped catheter (SPR 407; Millar Instruments) and advanced into the aorta and then into the LV for recording pressure and ±dP/dt.

Histological Analysis

After measurements, hearts were removed and cut into 2 transverse slices, and the basal specimens were fixed with 10% buffered formalin and embedded in paraffin. Sections 4-μm thick were stained with hematoxylin-eosin or Masson's trichrome. Quantitative assessments including cell size, cell population, and fibrotic area were performed using multipurpose color image processor LUZEX F (Nireco).

Western Blotting

An immunoprecipitation assay of the lysate of heart tissues was performed with Ultra-Link Biosupport medium (Pierce) using anti-Fas antibody and anti-Fas ligand antibody (both from BD Transduction Laboratories). Subsequently, the isolated protein was analyzed by Western blotting using the same antibodies. Sham-operated hearts 10 days after surgery, hearts with 10-day-old MI, normal thymus, and normal livers (n=5 each) were subjected to the assay.

Active forms of caspase-8 and caspase-3 were detected, respectively, using the primary antibody against caspase-8 (H-134; Santa Cruz Biotechnology) and caspase-3 (H-277; Santa Cruz Biotechnology) in sham-operated mice and LacZ gene-treated and sFas gene-treated mouse hearts with 10-day-old MI (n=5 each).

Hindlimb muscles of mice injected with Ad-LacZ or Ad.CAG-sFas 7 days earlier (n=3 each) were subjected to Western blot for exogenous sFas by anti-human IgG antibody (DAKO).

Immunohistochemical Analysis

The sections, 4-μm-thick deparaffinized sections or 8-μm-thick cryosections from the apical half of the ventricle, were incubated with anti-Fas antibody, anti-Fas ligand antibody, anti-Flk-1 antibody (Santa Cruz Biotechnology), anti-α-smooth muscle actin (SMA) antibody (Sigma), anti-CD45 antibody (Pharmingen), antimacrophage antibody (F4/80; Biomedicals AG), or anticardiac myosin heavy chain antibody (Santa Cruz Biotechnology). The ABC kit (DAKO) was used for the immunostaining of the deparaffinized sections with diaminobenzidine as the chromogen. For immunofluorescence of cryosections, Alexa Fluor 568 and 488 (Molecular Probes) were the secondary antibodies. Nuclei were counterstained with hematoxylin or Hoechst 33342. Sections were observed under a light, or confocal, microscope (LSM510; Zeiss).

In Situ Nick End-Labeling (TUNEL) and DNA Gel Electrophoresis

The TUNEL assay was performed in sections using an ApopTag kit (Intergene) principally according to the instructions of the supplier. Mammary tissue of mice was used as the positive control.

DNA extraction from cardiac tissue and subsequent electrophoresis were performed as reported previously.[14]

Electron Microscopy

Two to 3 animals in each group were used exclusively for transmission electron microscopic examinations after the hemodynamic examination. After perfusion fixation with phosphate-buffered 2.5% glutaraldehyde, pH 7.4, for 30 minutes, they were immersion-fixed in the same fixative overnight, postfixed with 1% osmium tetroxide for 1 hour, dehydrated through a graded series of ethanol, and embedded in Epon medium. Ultrathin sections were stained with

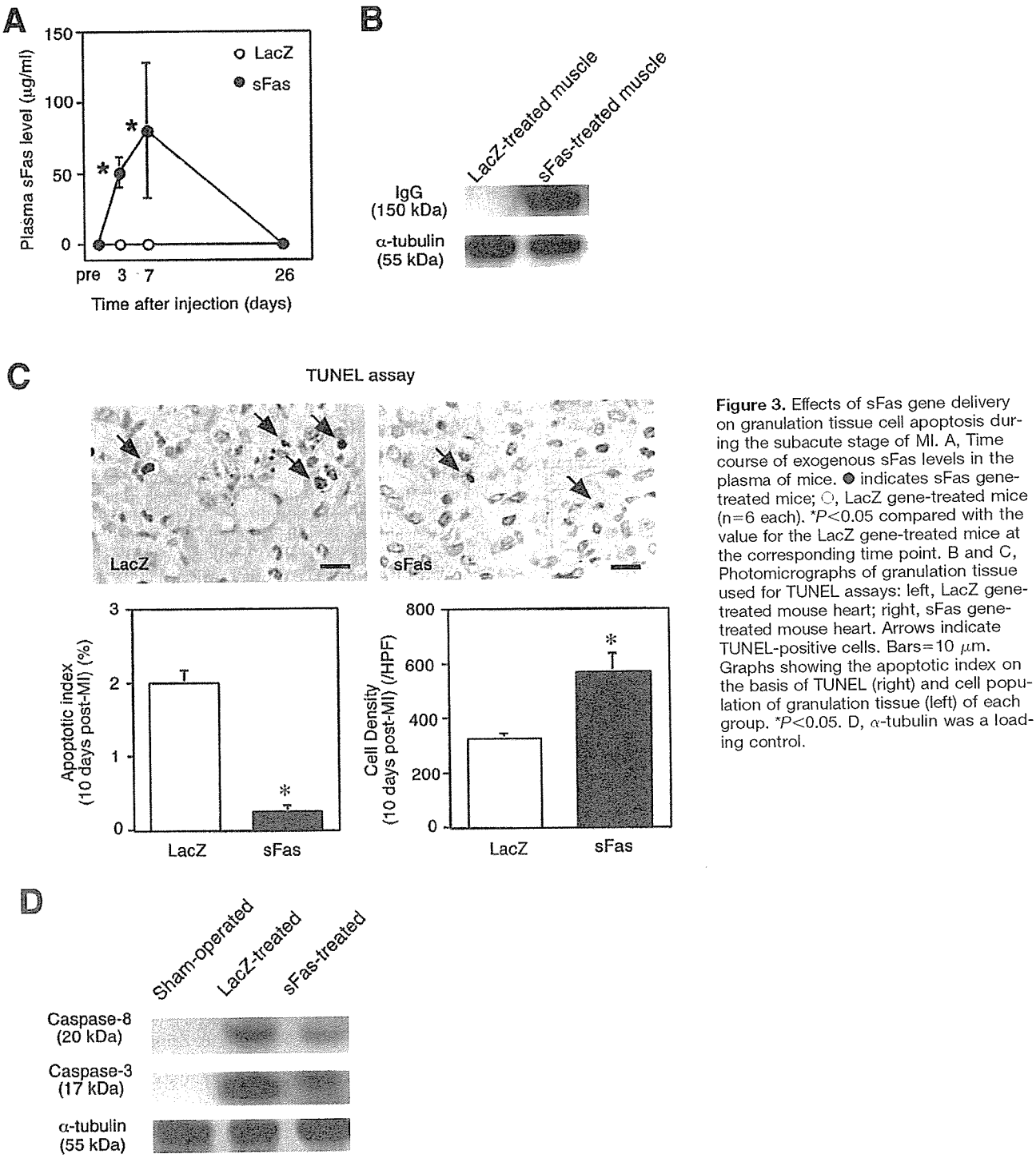

Figure 3. Effects of sFas gene delivery on granulation tissue cell apoptosis during the subacute stage of MI. A, Time course of exogenous sFas levels in the plasma of mice. ● indicates sFas gene-treated mice; ○, LacZ gene-treated mice (n=6 each). *$P<0.05$ compared with the value for the LacZ gene-treated mice at the corresponding time point. B and C, Photomicrographs of granulation tissue used for TUNEL assays: left, LacZ gene-treated mouse heart; right, sFas gene-treated mouse heart. Arrows indicate TUNEL-positive cells. Bars=10 μm. Graphs showing the apoptotic index on the basis of TUNEL (right) and cell population of granulation tissue (left) of each group. *$P<0.05$. D, α-tubulin was a loading control.

uranyl acetate and lead citrate and observed in an electron microscope (H700; Hitachi).

Statistical Analysis

Values are shown as mean±SEM. Analyses of survival after the third or tenth day after MI were performed using the Kaplan–Meier method with the log-rank Cox–Mantel method. The significance of differences was evaluated with Student *t* test, and a difference at $P<0.05$ was considered significant.

Results

Expression of Fas and Fas Ligand in Granulation Tissue Cells During MI

We first examined the expression of Fas and Fas ligand in granulation tissue of the heart at the subacute stage of MI (10 days after MI and 10 days after sham operation; n=5 each). Western blot analysis of the cardiac tissue revealed an

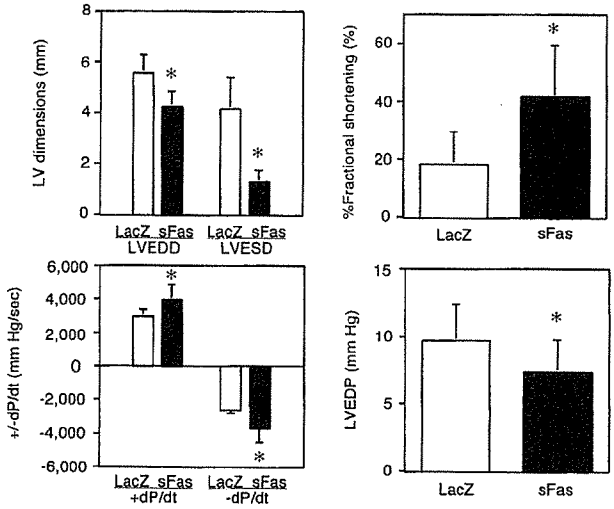

Figure 4. Effects of sFas gene delivery on hearts at the chronic stage of MI (4 weeks after MI). Graphs show anatomical and hemodynamic data obtained from echocardiography and cardiac catheterization. *$P<0.05$ compared with LacZ gene-delivered mice. LVEDD indicates LV end-diastolic dimension; LVESD, LV end-systolic dimension.

augmented expression of Fas and Fas ligand in the heart with MI (Figure 1A). Under a confocal microscope, Fas was identified on the plasma membrane of endothelial cells (Fas positivity 81±2.9% of the endothelial cells), vascular smooth muscle cells (69±2.0%), extravascular myofibroblasts (45±2.9%), macrophages (79±3.2%), and leukocytes (73±3.6%), whereas Fas ligand was found only on the plasma membrane of leukocytes (Fas ligand positivity 21±2.7% of the CD45-positive cells; Figure 1B). Under the present staining conditions, neither Fas nor Fas ligand was detected on the surface of cardiomyocytes, even at the border of the infarct area (Figure 1B).

Apoptosis was detectable by TUNEL assay in noncardiomyocytes of granulation tissue but never in cardiomyocytes. We failed to detect a ladder pattern on DNA gel electrophoresis in the tissue from hearts with 10-day-old MI (data not shown). This failure was compatible with previous reports[14,22] and was probably attributable to the relatively low incidence of apoptotic cells. Electron microscopy confirmed this finding, being compatible with previous studies:[14,15] apoptosis of noncardiomyocytes and no apoptosis of cardiomyocytes (data not shown).

Attenuated Postinfarction Heart Failure in Mice with Nonfunctioning Fas and Fas Ligand

MI was induced in animals with a nonfunctioning Fas (*lpr* strain: *fas*$^{-/-}$; n=10),[23] those with a nonfunctioning Fas ligand (*gld* strain: *fas ligand*$^{-/-}$; n=10),[24] and in the syngenetic control mice (C57BL/6J strain; n=10). The lack of Fas and Fas ligand was confirmed, respectively, in the hearts of the *lpr* strain and the *gld* strain mice 10 days after MI (data not shown). On the basis of the TUNEL assay, granulation tissue cell apoptosis in surviving mice with 10-day-old MI was significantly suppressed in the nonfunctioning Fas/Fas ligand strains (0.74±0.02% in the *lpr* strain [n=9] and 0.88±0.06% in the *gld* strain [n=9]) compared with the control (2.3±0.16%; n=8; Figure 2A). Next, MI was similarly evoked in the *lpr* strain, *gld* strain, and control (n=10 each), and followed up for 4 weeks. At the chronic stage (4 weeks after MI), echocardiographic and hemodynamic examinations of the surviving mice (9 *lpr* mice, 10 *gld* mice, and 7 control mice) revealed a significant attenuation of LV remodeling and improvement of LV dysfunction in the *lpr* and *gld* strains, compared with the control (Figure 2B).

To check the possible difference in magnitude of acute MI between the control and nonfunctioning Fas/Fas ligand mice, we histologically measured the acute infarct size 2 days after MI (n=6 each). There was no difference in the percentage of MI in LV area among the groups (Figure 2C). Also, there was no difference in the degree of acute inflammatory cell infiltration at the periphery of the 2-day-old infarct area (Figure 2C).

Inhibition of Granulation Tissue Cell Apoptosis by sFas, an Inhibitor of Fas-Mediated Apoptosis

MI was induced in 12-week-old male C57BL/6J mice, and Ad.CAG-sFas (10^9 pfu/mouse) was delivered systemically through injection into the hindlimbs on the third day after MI (n=10) when cardiomyocyte necrosis was already completed. The control gene was LacZ cDNA (Ad.CAG-LacZ; n=10). In the sFas gene–delivered mice, the plasma level of exogenous sFas reached 51.0±11.0 μg/mL and 80.7±4.7 μg/mL, respectively, 3 and 7 days after the injection (6 and 10 days after MI), when the infarct area consisted of granulation tissue (Figure 3A); these levels might be sufficiently high when considering that in humans, the normal level of plasma sFas is ≈2 ng/mL.[25] However, the exogenous sFas was undetectable in the plasma at 4 weeks after MI. We confirmed expression of exogenous sFas by Western blotting for human IgG in the hindlimb muscles injected with Ad.CAG-sFas 7 days earlier, but it was not detected in those treated with Ad-LacZ (Figure 3B).

The sFas gene treatment significantly reduced the incidence of TUNEL-positive cells in the infarct area consisting of granulation tissue (Figure 3C); the apoptotic index on the basis of TUNEL in the infarct area of the treated mice 10 days after MI was 0.24±0.09% compared with 2.0±0.18% for the control mice. Active forms of caspase-8 and caspase-3 were detected not in the sham-operated mouse hearts but in the hearts with 10-day-old MI. However, these signals were apparently attenuated in the hearts treated with the sFas gene (Figure 3D). The noncardiomyocyte population in the infarct area was significantly greater in the sFas-treated mice (569±67 cells/high-power field [HPF]) than in the LacZ-treated mice (324±19 cells/HPF; Figure 3C). The number of vessels, the %area of myofibroblasts, and the number of macrophages in the infarct was significantly greater in the sFas-treated group than in the LacZ-treated group: vessels (vessels/HPF) 231±19 versus 168±16, $P=0.0022$; myofibroblasts (%) 31.5±6.4 versus 17.8±2, $P=0.0076$; and macrophages (cells/HPF) 7.5±0.66 versus 4.5±0.38, $P=0.0024$. These findings suggest that the inhibition of apoptosis through the blocking Fas/Fas ligand interaction resulted in preservation of the postinfarct granulation tissue cell population.

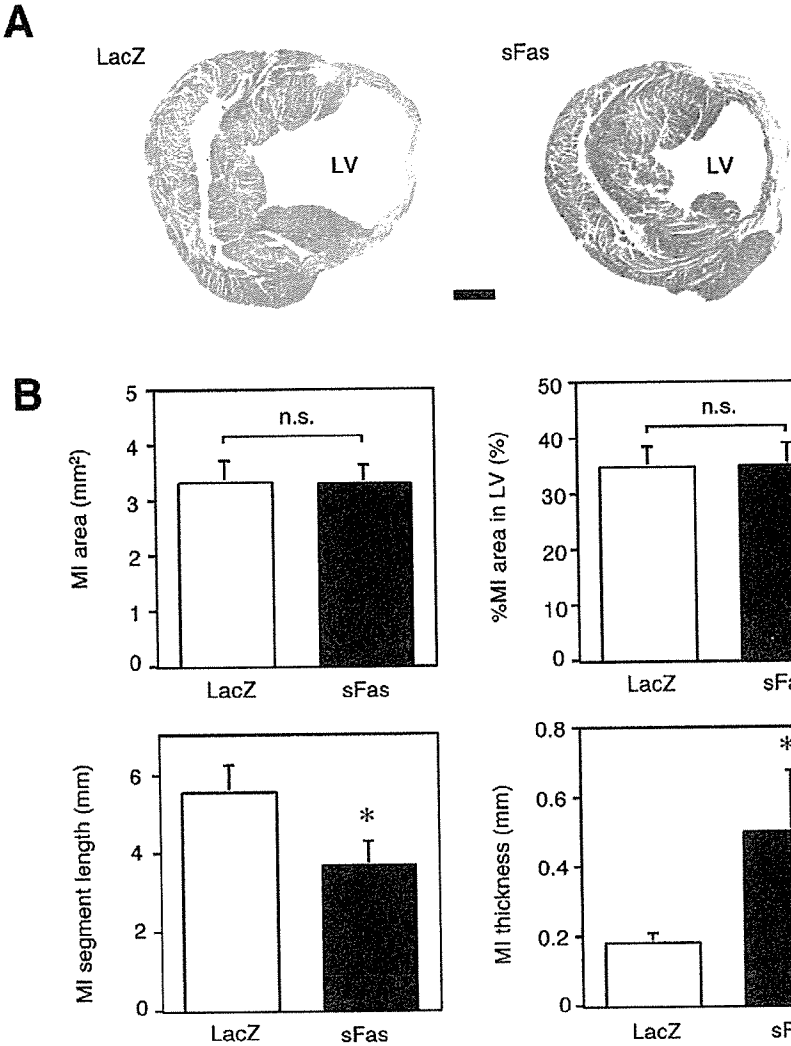

Figure 5. Effects of sFas gene delivery on hearts at the chronic stage of MI (4 weeks after MI). A, Transverse sections of hearts with 4-week-old MI; hematoxylin-eosin stain. Bar=1 mm. B, Graphs showing the absolute infarct area (μm^2); the percentage of the infarct area in total LV area (%); the length of the infarct segment (the inner circumferential length; μm); and the thickness of the infarct wall. *$P<0.05$ compared with the LacZ gene-delivered mice.

Improvement of Postinfarction LV Remodeling and Heart Failure by the sFas Gene Delivery

The influence of the sFas gene therapy was examined 4 weeks after MI (sFas gene [n=8] and LacZ gene [n=6]). At the chronic stage of MI, the LacZ-treated mice showed severe LV remodeling with a marked LV dilatation accompanying a thin infarct segment and signs of decreased cardiac function: decreased LV%FS and $\pm dP/dt$; and an increased LV end-diastolic pressure. Gene delivery on the third day of MI resulted in a significant improvement of each of these conditions (Figure 4). Systemic blood pressure and heart rate were similar between the LacZ-treated and sFas-treated groups. Treatment with the sFas gene in normal mice did not cause any hemodynamic alteration or morphological change in the hearts compared with the LacZ treatment (n=5 each; data not shown).

Necropsy of the hearts of mice at 4 weeks after MI revealed a severely dilated LV cavity with a thin infarct wall in the LacZ-treated group. However, this unfavorable LV remodeling appeared attenuated in the sFas-treated group (Figure 5A). The absolute infarct size and proportion of infarct area to total LV area were similar between the LacZ-treated and sFas-treated mice at 4 weeks after MI (Figure 5B). Interestingly, the wall thickness of the infarct segment was greater, whereas the inner circumferential length of the infarct segment was smaller in the sFas-treated mice (Figure 5B). This indicated that the remodeling of the infarct wall expanding in the coronal directions was significantly suppressed in the sFas-treated mice.

The 4-week-old infarct area of the LacZ-treated mice was replaced by fibrous scar tissue (Figure 6A). However, that of the sFas-treated mice contained not only collagen fibers and fibroblasts but also many small vessels and abundant extravascular α-SMA–positive cells (myofibroblasts). The population of noncardiomyocytes in the old infarct area was significantly greater in the sFas-treated mice (390 ± 9 cells/HPF in the sFas group versus 259 ± 9 cells/HPF in the control) and so was that of vessels (165 ± 7 vessels/HPF in the sFas group versus 114 ± 7 vessels/HPF in the control; Figure 6A). The percent area of extravascular α-SMA–positive cells was significantly greater in the sFas-treated group ($18\pm1.7\%$) than in the LacZ-treated group ($7.6\pm1.6\%$). Some α-SMA–positive cells accumulated and formed bundles running parallel to the surviving cardiomyocytes. Such bundles were not

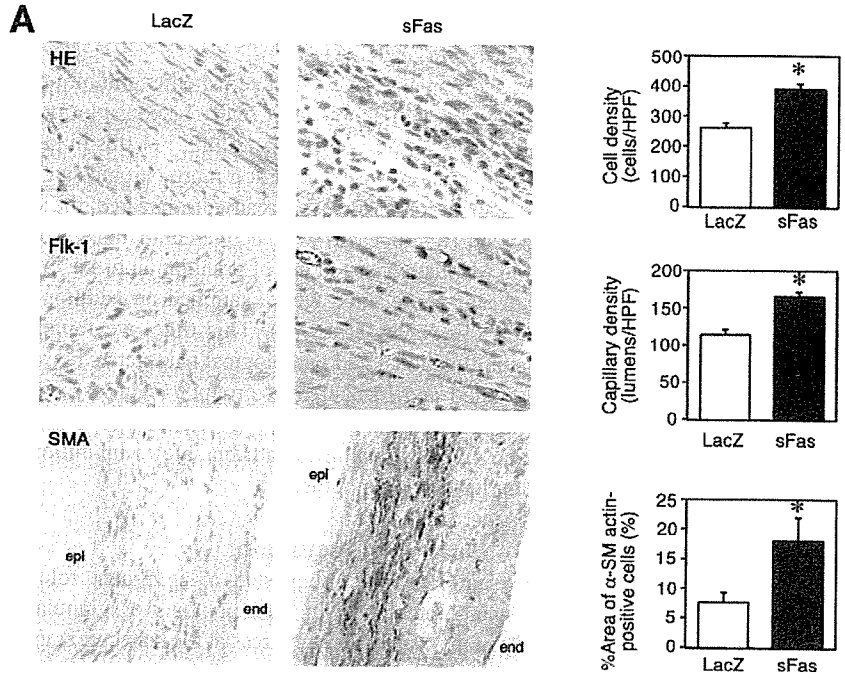

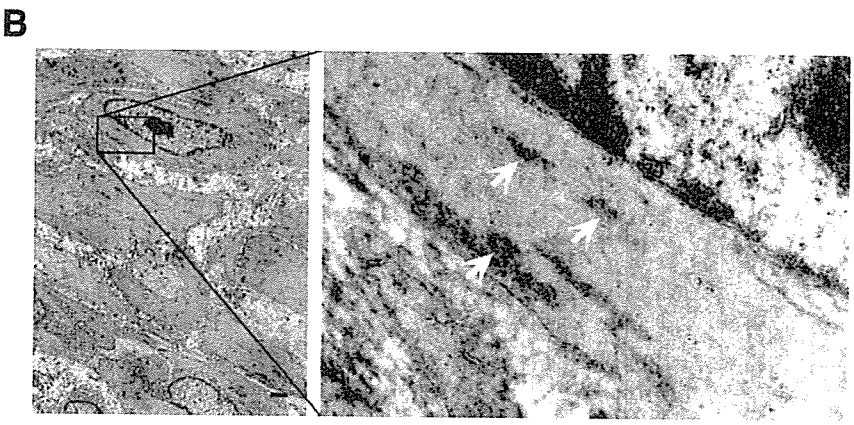

Figure 6. Effects of sFas gene delivery on cardiac histology and ultrastructure at the chronic stage of MI (4 weeks after MI). A, Photographs of histological and immunohistochemical preparations with graphs showing morphometrical data: the cell population of nonmyocytes in old infarct areas (cells/HPF); the vessel population in old infarct areas (vessels/HPF); and the percent areas of α-SMA–positive cells (%). *$P<0.05$ compared with the LacZ gene–delivered mice. B, Bundles of cells found in extravascular areas were found to be smooth muscle cells with a contractile phenotype under the electron microscope. The right panel is a highly magnified photograph of the squared portion of the neighboring panel showing densely packed myofilaments and dense bodies (arrows) in the cytoplasm. Bar=1 μm.

observed in the infarct wall of the LacZ-treated mice. However, macrophages were scarce even in the infarct area of the sFas-treated mouse hearts, and the incidence (1.7±0.62 cells/HPF) was similar to that in the LacZ-treated mice (1.3±0.56 cells/HPF; $P=0.6964$). The size of cardiomyocytes in the noninfarct area, which was measured as the transverse diameter, was significantly greater in the LacZ-treated mice (17.7±0.3 μm) than sFas-treated (14.0±0.7 μm) mice, suggesting that the compensatory hypertrophy of cardiomyocytes was more developed in the LacZ-treated mice. There was no special difference in thickness or in the degree of fibrosis of the noninfarct LV wall between the groups. No histological abnormality was found in the extracardiac organs such as lungs, liver, intestines, and kidneys of the sFas-treated mice.

Under an electron microscope, 4-week-old infarct areas of LacZ-treated mouse hearts contained fibroblasts/myofibroblasts (mostly fibroblasts), scanty small vessels, and very few macrophages that were surrounded by massive collagen fibrils, being consistent with a scar tissue. However, those of the sFas-treated hearts contained more abundant cell components. They showed not only numerous fibroblasts/myofibroblasts and small vessels but also mature smooth muscle cells with the contractile phenotype. These smooth muscle cells made bundles in the extravascular areas. The cytoplasms of the smooth muscle cells were tightly filled with thin filaments and contained many dense bodies (Figure 6B). The bundles of such smooth muscle cells were identical to the mass of α-SMA–positive cells that had appeared under the light microscope.

Influence of the sFas Gene Delivery on Postinfarction Survival

Using other litters of mice that were alive on the third day of MI (n=40), the survival was followed up for a period of 10 weeks. Eighteen mice underwent the sFas gene therapy and 22 the LacZ gene therapy. The survival rate was 55% in the control and 83% in the sFas-treated group at 10 weeks after MI ($P=0.0834$; Figure 7). Although the difference was not significant, it was notable that in case of

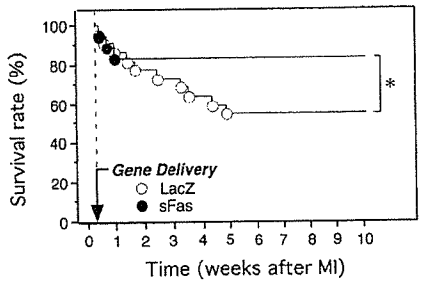

Figure 7. Survival of post-MI mice followed up for 10 weeks. ○ indicates LacZ gene treatment (n=20); ●, sFas gene treatment (n=18). *P=0.0834 (later than the third day of MI) or P=0.0389 (later than the tenth day of MI).

the sFas treatment, mice were all alive when survived for the first 10 days after MI. Thus, when the survival was evaluated later than 10 days after MI, the survival of sFas-treated mice was significantly better than that of the LacZ-treated mice (P=0.0389; Figure 7).

The echocardiographic and hemodynamic evaluations of the surviving mice revealed that the beneficial effects of sFas gene delivery on post-MI cardiac function were preserved, even up to 10 weeks after MI (Figure 8). The necropsy study revealed that the greater MI wall thickness and smaller MI segmental length in the sFas-treated group was preserved (Figure 8). These findings indicate that the effect of sFas gene therapy persisted for many weeks, even after the exogenous sFas level had become undetectable.

Ineffectiveness of the sFas Gene Delivery During the Chronic Stage of MI

In further experiments, we checked whether inhibition of granulation tissue cell apoptosis is really responsible for the beneficial effects on post-MI heart failure. For this purpose, the sFas gene therapy was started at a more chronic stage of MI when granulation tissue has already disappeared; the sFas or LacZ gene (n=10 each) was delivered to mice with a 6-week-old MI that consisted not of granulation tissue but of scar tissue, and these mice were examined an additional 4 weeks later (10 weeks after MI). This time, we found no difference in functional and pathological parameters between the sFas-treated and LacZ-treated groups (Figure 8). These results clearly indicate that the preventive effect of the sFas gene therapy on heart failure is attributable to inhibition of granulation tissue cell apoptosis.

Discussion

In the present study, we suggested a significant role for Fas/Fas ligand interaction in the apoptosis of granulation tissue cells in myocardial infarct areas at the subacute stage of MI. Granulation tissue cells disappear naturally via apoptosis to eventually make a scar tissue.[14] The present study revealed that suppression of granulation tissue cell apoptosis by interfering with the Fas/Fas ligand interaction through sFas gene delivery resulted: anatomically, in attenuation of unfavorable remodeling of the LV; and functionally, in amelioration of cardiac dysfunction at the chronic stage of MI.

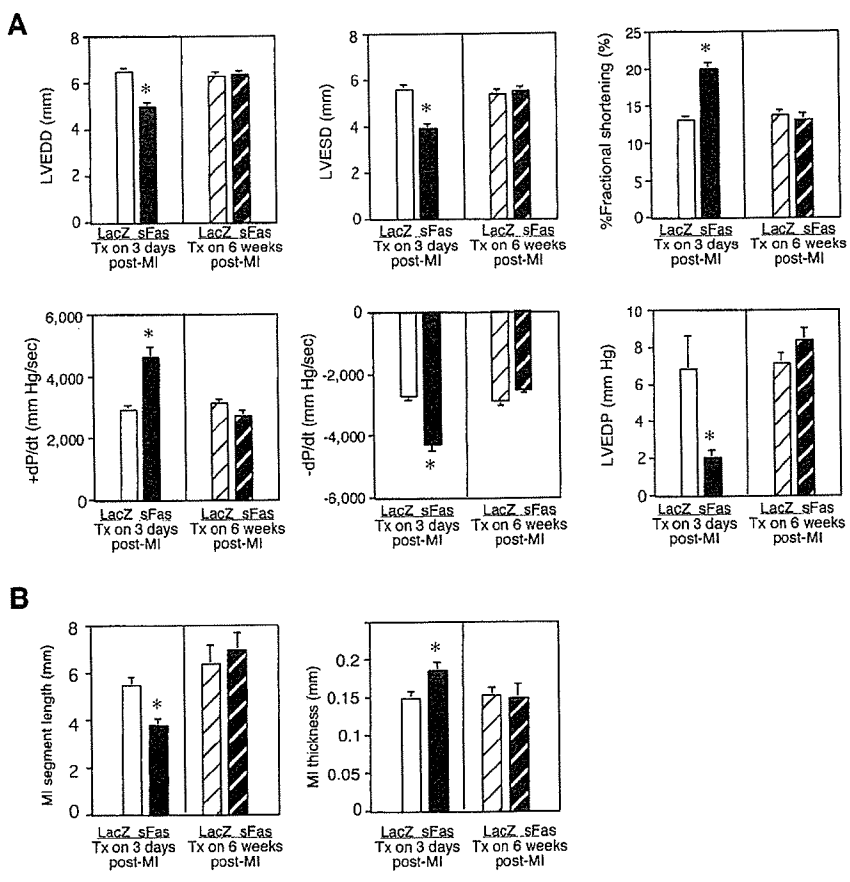

Figure 8. sFas gene delivery was effective even 10 weeks after MI, when it was applied at the subacute stage of MI (3 days after MI), whereas it was ineffective when applied at the chronic stage of MI (6 weeks after MI). Graphs show anatomical, hemodynamic, and pathological data for hearts at the chronic stage of MI (10 weeks after MI) obtained from echocardiography, cardiac catheterization, and necropsy study. *P<0.05 compared with the LacZ gene–delivered mice.

Post-MI survival during the chronic stage (later than the subacute stage) was also affected by the treatment. The results of the treatment were interesting, especially in terms of cardiac structure at the chronic stage: a thickened infarct wall developed containing abundant cellular components such as vessels and α-SMA–positive cells, part of which were found to be contractile phenotype smooth muscle cells under an electron microscope. The following are mechanistic considerations of the beneficial effects of the inhibition of granulation tissue cell apoptosis. First, the influence of infarct tissue geometry may be most important (ie, the shortening of the infarct segment length and increase in the infarct wall thickness). Contraction of the infarct tissue contributes to the suppression of ventricular dilatation. Because wall stress is proportional to the cavity diameter and inversely proportional to the wall thickness (Laplace's law),[26] and because wall stress and ventricular remodeling (dilatation) have a vicious relationship, accelerating each other, it is conceivable that such an alteration of infarct tissue geometry would bring a marked benefit of improving the hemodynamic state. Also, a smaller aneurysm has a lesser effect on cardiac function. Second, bundles of smooth muscle cells with a contractile phenotype in the infarct area, running in parallel with the surviving myocytes, might aid the global contractility of the LV. Third, the preservation of vessels might relieve ischemia in the surviving tissue. On the other hand, inhibition of cardiomyocyte apoptosis was not considered important because of the lack of TUNEL-positive cardiomyocytes during the subacute stage of MI, even in the LacZ-treated hearts. Compensatory hypertrophy of cardiomyocytes was independent of the beneficial effects because the cardiomyocytes were smaller in the sFas-treated than LacZ-treated hearts.

Although we showed the beneficial effect of the inhibition of granulation tissue apoptosis after MI, it should be cautioned that the benefit was evident in cases with large, transmural infarcts; the outcome would be unknown if the therapy were applied to cases with subendocardial infarction.

In the present study, we suggested that the apoptosis of each cell type of postinfarction granulation tissue is, at least in part, Fas dependent. However, macrophages continued to die, whereas vascular endothelial cells and myofibroblasts, having escaped a strong proapoptotic environment (granulation tissue as an inflammatory focus) by antiapoptotic treatment (sFas gene therapy), might continue to live until later. Speculatively, macrophages may have a higher sensitivity to apoptotic stimuli compared with the other preserved cells because inflammatory cells generally show very active proapoptotic interactions through death ligands and receptors.[16]

Fas was not immunohistochemically detected in cardiomyocytes under the present staining conditions. However, immunohistochemical negativity does not always deny the slight expression of an antigen because the sensitivity depends on the staining conditions. Several previous reports have shown immunohistochemically Fas expression in the cardiomyocytes of rats[27,28] and of humans.[29] Thus, it may be possible that our immunostaining method for Fas was less sensitive compared with those used in the previous studies. Notwithstanding, we detected Fas expression in the granulation tissue cells. This fact indicates that Fas expression in granulation tissue cells is definitely stronger than that in cardiomyocytes and suggests that the role of the Fas/Fas interaction in granulation tissue cells may be more significant than that in cardiomyocytes.

Postinfarct heart failure affects nearly half of all candidates for cardiac transplantation[30] and is one of the most serious clinical problems to be overcome in cardiovascular medicine. Recently, we reported that the inhibition of granulation tissue cell apoptosis by a pancaspase inhibitor after MI had beneficial effects on cardiac remodeling and dysfunction at the chronic stage of MI. The present study confirmed this therapeutic concept. However, because most of the apoptosis in a physiological setting is considered caspase dependent,[31] the systemic suppression of caspases may potentially have unfavorable effects on healthy organs. Actually, caspase 3-deficient homozygous mice undergo embryonic death.[32] On the basis of these facts, inhibition of the Fas/Fas ligand interaction may be a more specific way to apoptosis inhibition than inhibition of caspases. Our findings may warrant a therapeutic trial against postinfarction heart failure, which could be performed even during the subacute stage of MI in patients who have a large MI because the chance of reperfusion therapy during the acute stage has been lost. Thus, we expect the "inhibition of granulation tissue cell apoptosis" to become a novel therapeutic regimen that is prophylactic against chronic heart failure after large MI.

Acknowledgments

We thank Akiko Tsujimoto, Hatsue Ohshika, and the staff of Kyoto Women's University (Kaori Abe, Keiko Uodzu, Kazumi Ohara, Hitomi Takagaki, Machiko Mizutani, and Miyuki Morikawa) for technical assistance.

References

1. Pfeffer MA. Left ventricular remodeling after acute myocardial infarction. *Annu Rev Med.* 1995;46:455–466.
2. Reimer KA, Vander Heide RS, Richard VJ. Reperfusion in acute myocardial infarction: effect of timing and modulating factors in experimental models. *Am J Cardiol.* 1993;72:13G–21G.
3. McKay RG, Pfeffer MA, Pasternak RC, Markis JE, Come PC, Nakao S, Alderman JD, Ferguson JJ, Safian RD, Grossman W. Left ventricular remodeling after myocardial infarction: a corollary to infarct expansion. *Circulation.* 1986;74:693–702.
4. Weisman HF, Bush DE, Mannisi JA, Weisfeldt ML, Healy B. Cellular mechanisms of myocardial infarct expansion. *Circulation.* 1988;78:186–201.
5. Cheng W, Kajstura J, Nitahara JA, Li B, Reiss K, Liu Y, Clark WA, Krajewski S, Reed JC, Olivetti G, Anversa P. Programmed myocyte cell death affects the viable myocardium after infarction in rats. *Exp Cell Res.* 1996;226:316–327.
6. Shan K, Kurrelmeyer K, Seta Y, Wang F, Dibbs Z, Deswal A, Lee-Jackson D, Mann DL. The role of cytokines in disease progression in heart failure. *Curr Opin Cardiol.* 1997;12:218–223.
7. Olivetti G, Abbi R, Quaini F, Kajstura J, Cheng W, Nitahara JA, Quaini E, Di Loreto C, Beltrami CA, Krajewski S, Reed JC, Anversa P. Apoptosis in the failing human heart. *N Engl J Med.* 1997;336:1131–1141.
8. Narula J, Kolodgie FD, Virmani R. Apoptosis and cardiomyopathy. *Curr Opin Cardiol.* 2000;15:183–188.
9. Gill C, Mestril R, Samali A. Losing heart: the role of apoptosis in heart disease—a novel therapeutic target? *FASEB J.* 2002;16:135–146.
10. Elsässer A, Suzuki K, Schaper J. Unresolved issues regarding the role of apoptosis in the pathogenesis of ischemic injury and heart failure. *J Mol Cell Cardiol.* 2000;32:711–724.
11. Kang PM, Izumo S. Apoptosis and heart failure: a critical review of the literature. *Circ Res.* 2000;86:1107–1113.
12. Hayakawa K, Takemura G, Koda M, Kawase Y, Maruyama R, Li Y, Minatoguchi S, Fujiwara T, Fujiwara H. Sensitivity to apoptosis signal,

clearance rate, and ultrastructure of Fas ligand-induced apoptosis in in vivo adult cardiac cells. *Circulation*. 2002;105:3039–3045.
13. Kostin S, Pool L, Elsässer A, Hein S, Drexler HC, Arnon E, Hayakawa Y, Zimmermann R, Bauer E, Klovekorn WP, Schaper J. Myocytes die by multiple mechanisms in failing human hearts. *Circ Res*. 2003;92: 715–724.
14. Takemura G, Ohno M, Hayakawa Y, Misao J, Kanoh M, Ohno A, Uno Y, Minatoguchi S, Fujiwara T, Fujiwara H. Role of apoptosis in the disappearance of infiltrated and proliferated interstitial cells after myocardial infarction. *Circ Res*. 1998;82:1130–1138.
15. Hayakawa K, Takemura G, Kanoh M, Li Y, Koda M, Kawase Y, Maruyama R, Okada H, Minatoguchi S, Fujiwara T, Fujiwara H. Inhibition of granulation tissue cell apoptosis during the subacute stage of myocardial infarction improves cardiac remodeling and dysfunction at the chronic stage. *Circulation*. 2003;108:104–109.
16. Nagata S. Apoptosis by death factor. *Cell*. 1997;88:355–365.
17. Suda T, Hashimoto H, Tanaka M, Ochi T, Nagata S. Membrane Fas ligand kills human peripheral blood T lymphocytes, and soluble Fas ligand blocks the killing. *J Exp Med*. 1997;186:2045–2050.
18. Li Y, Takemura G, Kosai K, Yuge K, Nagano S, Esaki M, Goto K, Takahashi T, Hayakawa K, Koda M, Kawase Y, Maruyama R, Okada H, Minatoguchi S, Mizuguchi H, Fujiwara T, Fujiwara H. Postinfarction treatment with adenoviral vector expressing hepatocyte growth factor relieves chronic left ventricular remodeling and dysfunction in mice. *Circulation*. 2003;107:2499–2506.
19. Mizuguchi H, Kay AM. A simple method for constructing E1- and E1/E4-deleted recombinant adenoviral vectors. *Hum Gene Ther*. 1999; 10:2013–2017.
20. Suda T, Nagata S. Purification and characterization of the Fas-ligand that induces apoptosis. *J Exp Med*. 1994;179:873–879.
21. Chen SH, Chen XH, Wang Y, Kosai K, Finegold MJ, Rich SS, Woo SL. Combination gene therapy for liver metastasis of colon carcinoma in vivo. *Proc Natl Acad Sci USA*. 1995;92:2577–2581.
22. Desmouliere A, Redard M, Darby I, Gabbiani G. Apoptosis mediates the decrease in cellularity during the transition between granulation tissue and scar. *Am J Pathol*. 1995;146:56–66.
23. Watanabe-Fukunaga R, Brannan CI, Copeland NG, Jenkins NA, Nagata S. Lymphoproliferation disorder in mice explained by defects in Fas antigen that mediates apoptosis. *Nature*. 1992;356:314–317.
24. Takahashi T, Tanaka M, Brannan CI, Jenkins NA, Copeland NG, Suda T, Nagata S. Generalized lymphoproliferative disease in mice, caused by a point mutation in the Fas ligand. *Cell*. 1994;76:969–976.
25. Nishigaki K, Minatoguchi S, Seishima M, Asano K, Noda T, Yasuda N, Sano H, Kumada H, Takemura M, Noma A, Tanaka T, Watanabe S, Fujiwara H. Plasma Fas ligand, an inducer of apoptosis, and plasma soluble Fas, an inhibitor of apoptosis, in patients with chronic congestive heart failure. *J Am Coll Cardiol*. 1997;29:1214–1220.
26. Yin FC. Ventricular wall stress. *Circ Res*. 1981;49:829–842.
27. Kajstura J, Cheng W, Reiss K, Clark WA, Sonnenblick EH, Krajewski S, Reed JC, Olivetti G, Anversa P. Apoptotic and necrotic myocyte cell deaths are independent contributing variables of infarct size in rats. *Lab Invest*. 1996;74:86–107.
28. Wollert KC, Heineke J, Westermann J, Ludde M, Fiedler B, Zierhut W, Laurent D, Bauer MK, Schulze-Osthoff K, Drexler H. The cardiac Fas (APO-1/CD95) Receptor/Fas ligand system: relation to diastolic wall stress in volume-overload hypertrophy in vivo and activation of the transcription factor AP-1 in cardiac myocytes. *Circulation*. 2000;101: 1172–1178.
29. Filippatos G, Leche C, Sunga R, Tsoukas A, Anthopoulos P, Joshi I, Bifero A, Pick R, Uhal BD. Expression of FAS adjacent to fibrotic foci in the failing human heart is not associated with increased apoptosis. *Am J Physiol*. 1999;277:H445–H451.
30. Hosenpud JD, Bennett LE, Keck BM, Boucek MM, Novick RJ. The registry of the International Society for Heart and Lung Transplantation: seventeenth official report-2000. *J Heart Lung Transplant*. 2000;19: 909–931.
31. Thornberry NA, Lazebnik Y. Caspases: enemies within. *Science*. 1998; 281:1312–1316.
32. Kuida K, Zheng TS, Na S, Kuan C, Yang D, Karasuyama H, Rakic P, Flavell RA. Decreased apoptosis in the brain and premature lethality in CPP32-deficient mice. *Nature*. 1996;384:368–372.